2,3,9- and 2,3,11-Trisubstituted Tetrahydroprotoberberines as D_2 Dopaminergic Ligands

Javier Párraga [a], Nuria Cabedo [b], Sebastián Andujar [c], Laura Piqueras [d], Laura Moreno [a], Abraham Galán [a], Emilio Angelina [c], Ricardo D. Enriz [c], María Dolores Ivorra [a], María Jesús Sanz [d,e] and Diego Cortes [a,*]

[a]*Departamento de Farmacología, Laboratorio de Farmacoquímica, Facultad de Farmacia, Universidad de Valencia, 46100 Burjassot, Valencia, Spain*
[b]*Centro de Ecología Química Agrícola-Instituto Agroforestal Mediterráneo, Universidad Politécnica de Valencia, Campus de Vera, Edificio 6C, 46022 Valencia, Spain*
[c]*Departamento de Química, Universidad Nacional de San Luís, Argentina*
[d]*Departamento de Farmacología, Facultad de Medicina, Universidad de Valencia, 46010 Valencia, Spain*
[e]*Institute of Health Research-INCLIVA, University Clinic Hospital of Valencia, Valencia, Spain.*

[*]Corresponding author: Tel.: (+34) 963.54.49.75; Fax: (+34) 963.54.49.43; dcortes@uv.es
www.farmacoquimicavalencia.es

Abstract

Dopamine-mediated neurotransmission plays an important role in relevant psychiatric and neurological disorders. Nowadays, there is an enormous interest in the development of new dopamine receptors (DR) acting drugs as potential new targets for the treatment of schizophrenia or Parkinson´s disease. Previous studies have revealed that isoquinoline compounds such as tetrahydroisoquinolines (THIQs) and tetrahydroprotoberberines (THPBs) can behave as selective D_2 dopaminergic alkaloids since they share structural similarities with dopamine. In the present study we have synthesized eleven 2,3,9- and 2,3,11-trisubstituted THPB compounds (six of them are described for the first time) and evaluated their potential dopaminergic activity. Binding studies on rat striatal membranes were used to evaluate their affinity and selectivity towards D_1 and D_2 DR and establish the structure-activity relationship (SAR) as dopaminergic agents. In general, all the tested THPBs with protected phenolic hydroxyls showed a lower affinity for D_1 and D_2 DR than their corresponding homologues with free hydroxyl groups. In previous studies in which dopaminergic affinity of 1-benzyl-THIQs (BTHIQs) was evaluated, the presence of a Cl into the A-ring resulted in increased affinity and selectivity towards D_2 DR. This is in contrast with the current study since the existence of a chlorine atom into the A-ring of the THPBs caused increased affinity for D_1 DR but dramatically reduced the selectivity for D_2 DR. An OH group in position 9 of the THPB (**9f**) resulted in a higher affinity for DR than its homologue with an OH group in position 11 (**9e**) (250 fold for D_2 DR). None of the compounds showed any cytotoxicity in freshly isolated human neutrophils. A molecular modeling study of three representative THPBs was carried out. The combination of MD simulations with DFT calculations provided a clear picture of the ligand binding interactions from a structural and energetic point of view. Therefore, it is likely that

compound **9d** (2,3,9-trihydroxy-THPB) behave as D_2 DR agonist since serine residues cluster are crucial for agonist binding and receptor activation.

Keywords: Tetrahydroprotoberberines, dopamine receptors, structure-activity relationships cytotoxicity, MTT and cytofluorometric analysis, theoretical calculations.

1. Introduction

Dopamine-mediated neurotransmission plays an important role in several psychiatric and neurological disorders affecting several million people worldwide. Researchers have focused their efforts in investigating the modulation of dopaminergic activity via the dopamine receptors (DR) as potential targets for treating schizophrenia or Parkinson´s disease. Therefore, there is an increased interest in the discovery of novel dopaminergic ligands as potential drug candidates in the therapy of these neurological disorders [1]. DR can be classified into two pharmacologic families (D_1 and D_2-like) that are encoded by at least five genes. From a therapeutical point of view, drugs acting at D_2-like DR are more relevant than those interacting with D_1-like DR [2]. In this context, whereas the D_2-like DR antagonists are used in the treatment of schizophrenia (antipsychotics), the agonists are used in the treatment of Parkinson's disease [1,3]. In addition, other studies have revealed the potential role of D_2 agonist in the treatment of depression. The pathophysiology of depression has been classically assigned to the noradrenaline and serotonine systems however, nowadays, published reports also support a role of the dopaminergic system in this disorder [2]. In regard to this, different selective D_2-type DR agonists were found to display antidepressant-like actions in several rodent models, suggesting a specific role of this receptor subtype in their antidepressant efficacy [4-8].

Previous studies from our group have revealed that isoquinoline compounds such as tetrahydroisoquinolines (THIQs) have affinity for DR in striate membranes of rat brain tissue which was likely due to their structural similarities to dopamine [8-18]. Likewise, tetrahydroprotoberberines (THPBs) are another group of natural and synthetic isoquinoline alkaloids with a variety of powerful biological activities, including

dopaminergic activity [19-21]. Indeed, coreximine, a natural tetrasubstituted THPB, and other analogues were reported as selective D_2 dopaminergic alkaloids [22]. Recently, l-stepholidine analogues have been synthetized displaying a dual dopaminergic activity, partial agonism at the D_1 DR and antagonism at D_2 DR [23].

Since THPBs, THIQs and dopamine share structural similarities, in the present study we have synthesized eleven 2,3,9- and 2,3,11-trisubstituted THPB compounds (six of them are here described for the first time) and evaluated their potential dopaminergic activity. Their structures were determined on the basis of their NMR spectral data and mass spectrometry analysis. The structural features that define the affinity and selectivity of the three series of THPBs synthesized for D_1/D_2 receptors was determined analyzing the influence of the substitution at the 2,3- and 9 or 11 positions, in order to obtain dopaminergic ligands with increased specificity. Therefore, all the synthesized compounds were tested for their ability to displace the selective radioligands of D_1 and D_2-like DR from their specific binding sites in striatal membranes in order to establish the structure-activity relationship (SAR) as dopaminergic agents. In addition, cytotoxicity studies in human cells were carried out. For this purpose, we used the MTT ((3-(4,5-Dimethylthiazol-2-yl)-2,5-diphenyltetrazolium bromide) assay and a cytofluorometric analysis to determine their impact on human neutrophil apoptosis and survival [24-26]. All of them were devoid of any toxic effect in these *in vitro* assays.

In order to better understand the molecular interactions stabilizing and destabilizing the different THPBs/D_2DR complexes, a molecular modelling study using molecular dynamic simulations and quantum mechanic calculations was carried out for the most representative compounds of this series. Thus, the possible stereo-electronic requirements of the THPBs/D_2 DR interactions have been discussed based on their different affinities.

2. Results and Discussion

In the present study, the impact of different substituents into the A- and D-ring of synthesized THPBs on dopaminergic affinity was evaluated. In previous reports, we determined the relevance of different substitutions into the A-ring in natural and synthetic isoquinoline alkaloids. We observed that the presence of hydroxyls groups in this ring caused increased affinity for the D_1-like and D_2-like DR families, while blockade of these hydroxyls groups resulted in decreased affinity [8,12-15]. Moreover, the presence of a halogen in the A-ring led to a selective binding at least to one of the two DR subtypes investigated [8,16,17]. Therefore, we have prepared three series of THPBs: 2,11-dihydroxy-3-chloro-THPB (series 1), 2,3-dihydroxy-11-methoxy-THPB (series 2) and 2,3,11-trihydroxy-THPB and 2,3,9-trihydroxy-THPB (series 3) and differently substituted analogues (**Figure 1**).

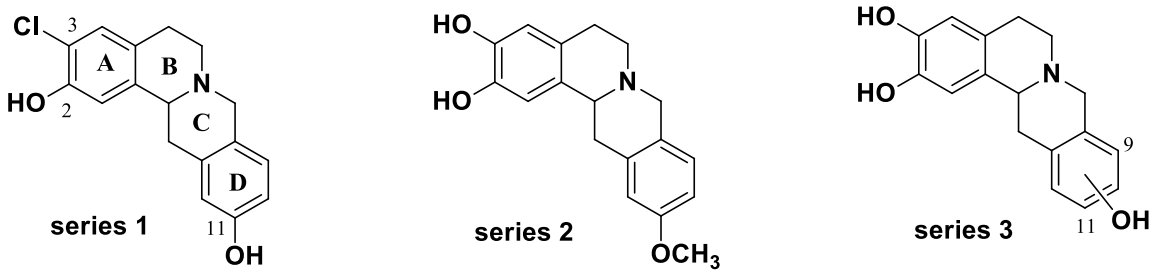

Figure 1. THPBs series.

Inasmuch, at the concentrations tested none of the synthesized THPBs affected human neutrophil apoptosis or survival, indicating the absence of cytotoxicity for human cells in these in vitro approaches. Molecular modelling of the possible stereo-electronic requirements for dopamine D_2 receptor ligands of the THPBs synthesized has been discussed based on the different affinities displayed.

2.1. Chemistry

The synthesis of the THPBs has been performed as outlined in the **Schemes 1**, **2** and **3**. The THPBs of the series 1 (**Scheme 1**) have been synthesized from 3-chloro-4-methoxybenzaldehyde as starting material. 3-Chloro-4-methoxy-β-nitroestyrene was obtained from 3-chloro-4-methoxybenzaldehyde by a Henry's reaction using nitromethane, ammonium acetate and acetic acid as solvent [27], and then, 3-chloro-4-methoxyphenylethylamine (**1**) was obtained by reduction with lithium aluminum hydride [28]. This phenylethylamine (**1**), was treated with 3-methoxyphenylacetyl chloride under Schotten-Baumann conditions to generate the *N*-(3-cloro-4-methoxyphenylethyl)-β-(3'-methoxyphenyl)acetamide (**2**) [29,30].

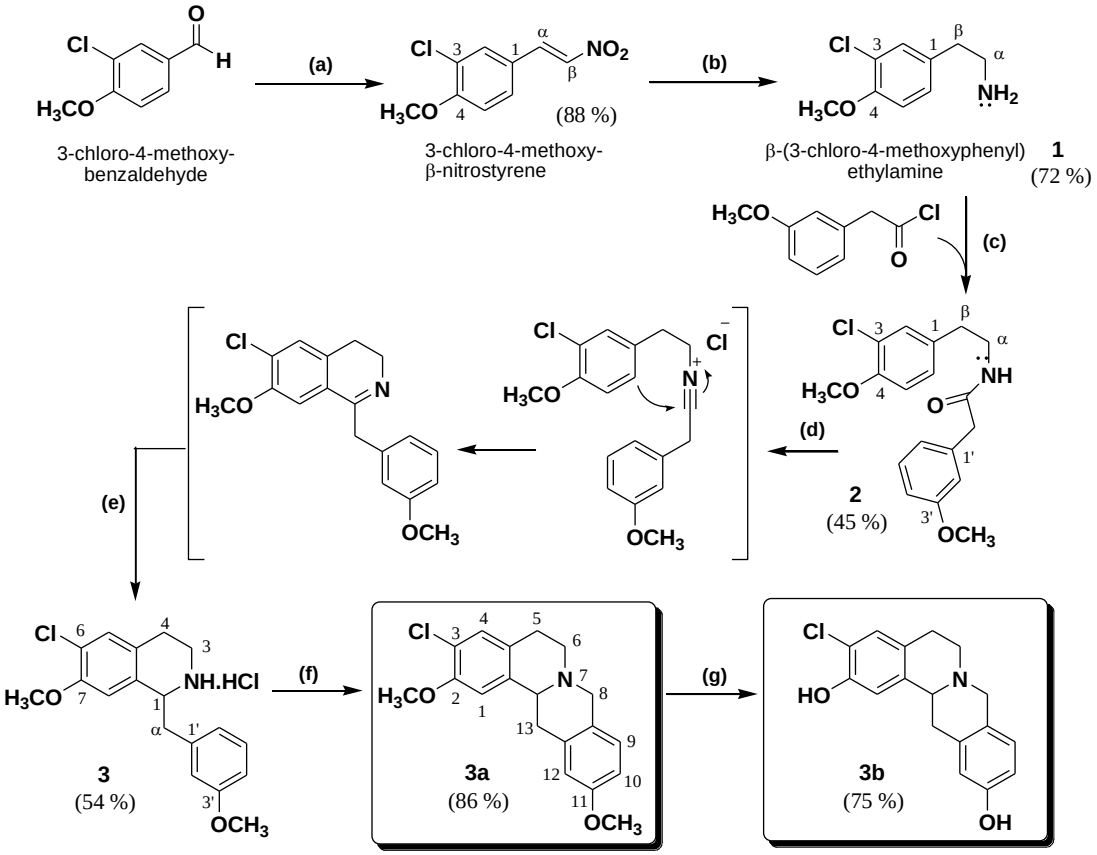

Scheme 1. Synthesis of THPBs **3a** and **3b** (Series 1). Reagents and Conditions: (a) Nitromethane, NH_4OAc, AcOH, reflux, 4h; (b) $LiAlH_4$, THF / Et_2O, N_2, reflux, 2h; (c) CH_2Cl_2, 3-methoxyphenylacetyl chloride, 5% NaOH, rt, 3h; (d) P_2O_5, $POCl_3$, Toluene, N_2, reflux, 8h; (e) $NaBH_4$; MeOH, rt, 2h; (f) HCHO, EtOH, H_2O, reflux, 5h; (g) CH_2Cl_2, BBr_3, rt, 2h.

Next, the phenylacetamide (**2**) was converted into the corresponding 1-benzyltetrahydroisoquinoline (BTHIQ) (**3**) using the Bischler-Napieralski cyclodehydration reaction. The use of a $POCl_3$ and P_2O_5 mixture in dry toluene followed by $NaBH_4$ reduction was required since the presence of a halogen in position 3 of the phenylacetamide can inactivate the Bischler-Napieralski cyclodehydration reaction due to the electro-attractive properties of the halogen [8,31-33]. Once obtained, the BTHIQ 6-chloro-7-methoxy-1-(3'-methoxybenzyl)-1,2,3,4-THIQ hydrochloride (**3**) was subjected to Mannich cyclization conditions using 37% aqueous formaldehyde [34] to generate the corresponding 2,11-dimethoxy-3-chloro-THPB (**3a**) with high yield (86%). Finally, the *O*-demethylation was performed by adding of 4 equivalents of BBr_3 reagent for 2 hours at room temperature [8] to obtain the 2,11-dihydroxy-3-chloro-THPB (**3b**) (**Scheme 1**).

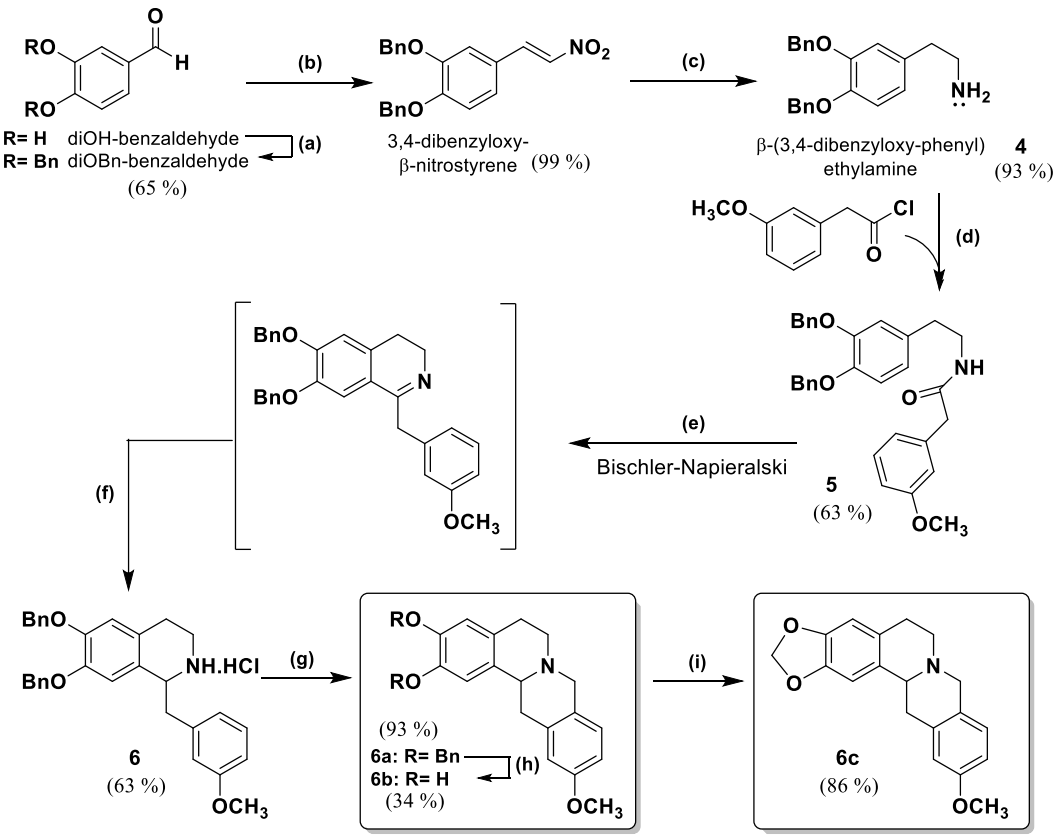

Scheme 2. Synthesis of THPBs **6a-6c** (Series 2). Reagents and Conditions: (a) Benzyl chloride, K_2CO_3, EtOH, reflux, 6h; (b) Nitromethane, NH_4OAc, AcOH, reflux, 4h; (c) $LiAlH_4$, THF / Et_2O, N_2, reflux, 2h; (d) CH_2Cl_2, 3-methoxyphenylacetyl chloride, 5% NaOH, rt, 3h; (e) $POCl_3$,

CH_3CN, N_2, reflux, 5h; (f) $NaBH_4$; MeOH, rt, 2h; (g) 37% HCHO, EtOH, H_2O, reflux, 5h; (h) EtOH-HCl, reflux, 3h; (i) DMF, CH_2Cl_2, CsF, reflux, 3h.

The THPBs of the series 2 (**Scheme 2**) have been synthesized using similar approaches to those previously described. A protective reaction of the hydroxyl groups was performed in 3,4-dihydroxybenzaldehyde through dibenzylation [28]. Once prepared the protected 3,4-dibenzyloxybenzaldehyde, a similar sequence of synthesis steps were carried out to obtain the phenylethylamine (**4**), the phenylacetamide (**5**), the BTHIQ (**6**) and finally, the corresponding 2,3-dibenzyloxy-11-methoxy-THPB (**6a**) with good yields (63-93%). In this series, the Bischler-Napieralski cyclodehydration was performed using only $POCl_3$ in dry acetonitrile since the presence of an alkoxy group in position 3 of the phenylacetamide can activate the Bischler-Napieralski cyclodehydration reaction due to the electro-donor ability of the oxygenated group. Then, this THPB was subjected to acidic conditions in absolute ethanol [12-35] in order to deprotect the phenolic hydroxyls groups yielding 2,3-dihydroxy-11-methoxy-THPB (**6b**). A methylendioxy group was generated by CsF and dichloromethane [13] from **6b** to obtain the 2,3-methylendioxy-11-methoxy-THPB (**6c**).

The THPBs of the series 3 (**Scheme 3**) have been synthesized employing similar procedures to those followed in series 1 and 2. The corresponding trisubstituted THPBs: 2,3,11-trimethoxy-THPB (**9a**) and 2,3,9-trimethoxy-THPB (**9b**) were obtained from 3,4-dimethoxyphenylethylamine (**7**). In this series, two different compounds were obtained based on the two possible positions of the Mannich cyclization. When cyclization was in *para* to the benzylic methoxy group, the 2,3,11-trimethoxy-THPB (**9a**) was the major product generated (77 % yield). In contrast, when cyclization occurred in *ortho* to the benzylic methoxy group then 2,3,9-trimethoxy-THPB (**9b**) was produced (8% yield). The phenolic hydroxyl groups were deprotected through *O*-demethylation conditions to

obtain the corresponding 2,3,11-trihydroxy-THPB (**9c**) and 2,3,9-trihydroxy-THPB (**9d**) respectively. Finally, the THPBs with methylendioxy group were prepared as above described to generate 2,3-methylendioxy-11-hydroxy-THPB (**9e**) and 2,3-methylendioxy-9-hydroxy-THPB (**9f**) respectively.

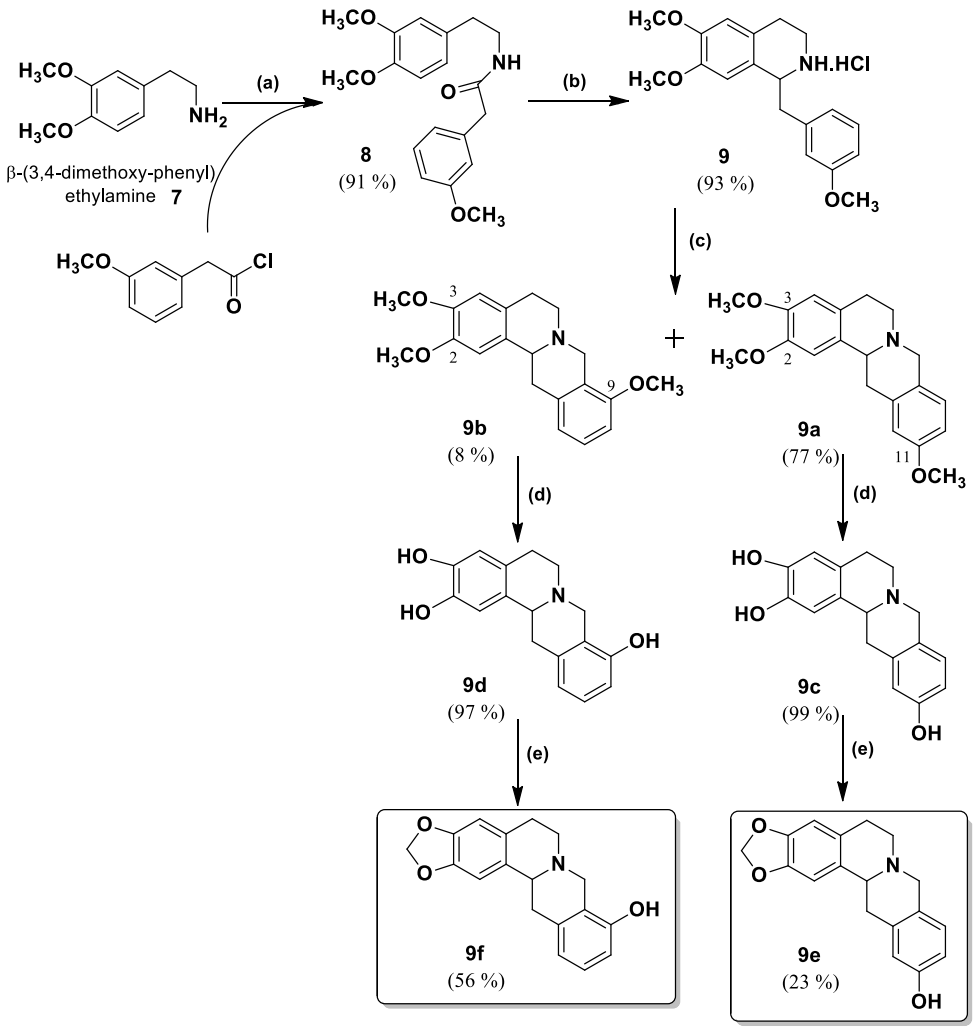

Scheme 3. Synthesis of THPBs **9a-9f** (Series 3). Reagents and Conditions: (a) CH_2Cl_2, 3-methoxyphenylacetyl chloride, 5% NaOH, rt, 3h; (b) $POCl_3$, CH_3CN, N_2, reflux, 5h; and, $NaBH_4$, MeOH, rt, 2h; (c) HCHO, EtOH, H_2O, reflux, 5h; (d) CH_2Cl_2, BBr_3, rt, 2h; (e) DMF, CH_2Cl_2, CsF, reflux, 3h.

2.2. Binding affinities for dopamine receptors: Structure-activity relationship

All the synthesized THPB compounds were assayed *in vitro* for their ability to displace the selective ligands of D_1 and D_2 DR from their respective specific binding sites in the striatal membranes. All the compounds except **6a**, were able to displace [^{3}H]-

SCH 23390 and [^{3}H]-raclopride from their specific binding sites at micromolar (µM) or nanomolar (nM) concentrations. This was not surprising given the bulky substituents (Bn) at C3 and C4 in compound **6a**. The binding affinities for D_1 and D_2 DR are summarized in **Table 1** illustrating some general trends of the structure-activity relationship.

Table 1
Values of affinity (K_i, pK_i) and selectivity (ratio Ki D_1/Ki D_2) determined in binding experiments to D_1 and D_2 DR of series 1-3.

	THPB	Specific ligand D_1 [^{3}H]-SCH 23390		Specific ligand D_2 [^{3}H]-raclopride		Ki D_1/D_2
		Ki (µM) [m]	pKi [m]	Ki (µM) [m]	pKi [m]	
3a	3-Cl-2,11-diMeO	1.813 ± 0.146	5.76 ± 0.09	2.046 ± 0.347	5.70 ± 0.07	0.9
3b	3-Cl-2,11-diOH	**0.107 ± 0.004**	**6.97 ± 0.02**[d,i]	0.188 ± 0.021	6.73 ± 0.05[b,i]	**0.6**
6a	2,3-diBnO-11-MeO	40.607 ± 4.215	4.39 ± 0.04[j]	40.866 ± 1.461	4.38 ± 0.02[j]	1.0
6b	2,3-diOH-11-MeO	1.108 ± 0.411	6.02 ± 0.17[e,h]	**0.078 ± 0.017**	**7.13 ± 0.09**[b,d,h]	**14.2**
6c	2,3-OCH_2O-11-MeO	2.373 ± 1.208	5.77 ± 0.27[f]	1.331 ± 0.536	5.94 ± 0.17[l]	1.8
9a	2,3,11-triMeO	4.314 ± 0.703	5. 38 ± 0.07	8.543 ± 4.709	5.29 ± 0.36	0.5
9b	2,3,9-triMeO	3.927 ± 0.908	5.44 ± 0.11	0.393 ± 0.115	6.44 ± 0.12[b,c,k]	**10**
9c	2,3,11-triOH	2.962 ± 1.042	5.58 ± 0.15	0.396 ± 0.028	6.41 ± 0.03[a]	7.5
9d	2,3,9-triOH	3.775 ± 0.992	5.46 ± 0.14	**0.093 ± 0.024**	**7.07 ± 0.14**[b,d]	**40.6**
9e	2,3-OCH_2O-11-OH	32.999 ± 5.009	4.49 ± 0.07[d]	7.506 ±1.591	5.16 ± 0.09[d]	4.4
9f	2,3-OCH_2O-9-OH	0.344 ± 0.027	6.47 ± 0.03[f,g]	**0.035 ± 0.012**	**7.55 ± 0.16**[a,f]	**10.0**

ANOVA, post Newmann-Keuls multiple comparison tests:
[a] $p < 0.05$ [b] $p < 0.01$, vs D_1-like DR.
[c] $p < 0.001$ vs **9a**. [d] $p < 0.001$ vs **9c**. [e] $p < 0.05$ vs **9c**. [f] $p < 0.001$ vs **9e**.
[g] $p < 0.001$ vs **9d**. [h] $p < 0.001$ vs **6a**, **6c**, **9a**. [i] $p < 0.001$ vs **3a**. [j] $p < 0.001$ vs **6b**.
[k] $p < 0.05$ vs **9d**. [l] $p < 0.01$ vs **9e**
[m] Data were displayed as mean ± SEM for 3-5 experiments.

2.2.1- Effect of the substituents into the A-ring of THPB

a) In general, all the tested THPBs with protected phenolic hydroxyls showed a lower affinity for D_1 and D_2 DR than their corresponding homologues with free hydroxyl groups (see **3a** vs **3b**, **6a** vs **6b**, **9a** vs **9c**, **9b** vs **9d** in **Table 1**). The higher

affinity for D_1 and D_2 DR of compounds with free phenolic group than those without was previously described albeit in several isoquinolines [8,12,16,21].

b) In previous studies in which dopaminergic affinity of BTHIQs was evaluated, the presence of a chlorine atom into the A-ring (*ortho* of oxygenated group) resulted in increased affinity and selectivity towards D_2 DR [8,16-18]. This is in contrast with the current study since the existence of a chlorine atom into the A-ring of the THPBs caused increased affinity for D_1 DR but dramatically reduced the selectivity for D_2 DR (see **3b** vs **9c** in **Tabla 1**).

c) Our results also showed that the presence of a methylenedioxy group in 2,3 position decreased the selectivity for D_2 DR (see **6c** vs **6b** and **9e** vs **9c** in **Table 1**). This effect was also observed when the substituent into the D-ring was in position 9. In fact, when the dopaminergic affinities of THPB **9d** (2,3,9-triOH) and **9f** (2,3-OCH_2O-, 9-OH) were compared, **9d** exerted higher selectivity for D_2 DR (Ki D_1/D_2 = 40.6) than **9f** (Ki D_1/D_2 = 10). Moreover, the latter compound (**9f**) is the THPB displaying the highest affinity for both DR types (Ki = 344 nM for D_1 and Ki = 35 nM for D_2) (see **Table 1** and **Figure 2**).

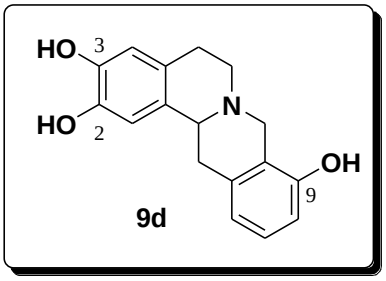

9d

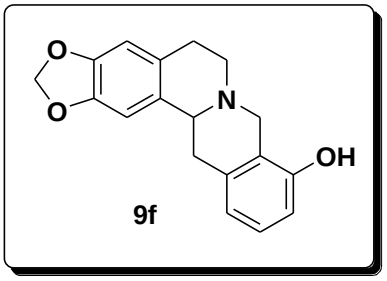

9f

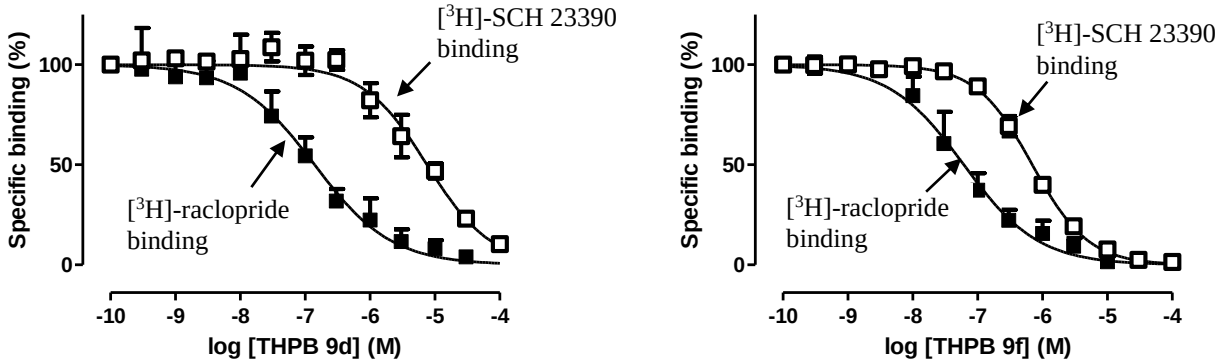

Figure 2. Displacement curves of [^{3}H]-SCH 23390 (D_1) and [^{3}H] raclopride (D_2) specific binding by compounds **9d** and **9f**. Data were displayed as mean ± SEM for 3-5 experiments.

2.2.2- Effect of the 9 or 11 substituent into the D-ring of THPB

The present study demonstrated that the affinity and the selectivity for DR depended on the position of the oxygenated substituents in positions 9 or 11 and on their protection or deprotection. In regard to this:

a) A hydroxyl group in position 9 of the THPB (**9f**) resulted in a higher affinity for D_1 and D_2 DR than its homologue with a hydroxyl group in position 11 (**9e**). In this context, the affinity for D_2 DR displayed by **9f** was 214 fold higher than **9e** (**Table 1** and **Figure 3**).

b) Surprisingly, either when this 2,3-methylenedioxy-11-OH-THPB (**9e**) was compared with the protected 2,3-methylenedioxy-11-OMe-THPB (**6c**), or when the 2,3,11-triOH-THPB (**9c**) was compared with the protected 2,3-diOH-11-OMe-THPB (**6b**), an increased affinity for D_1 and D_2 DR was observed with the 11-*O*-protected derivatives (**6c** and **6b,** see **Table 1** and **Figure 4**).

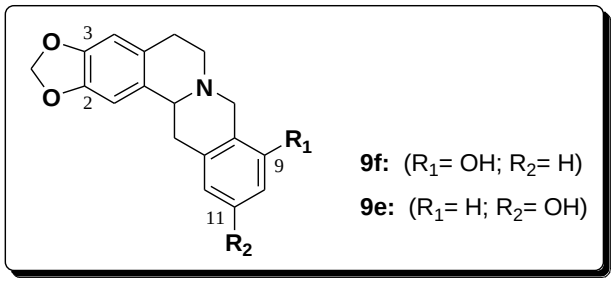

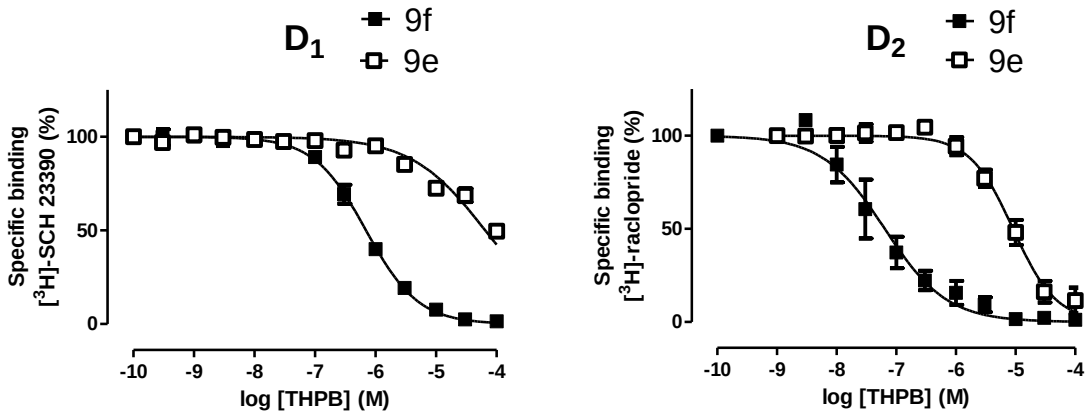

Figure 3. Displacement curves of the specific binding of D_1 and D_2 DR ligands by the compounds **9e** and **9f**. Data were displayed as mean ± SEM for 3-5 experiments.

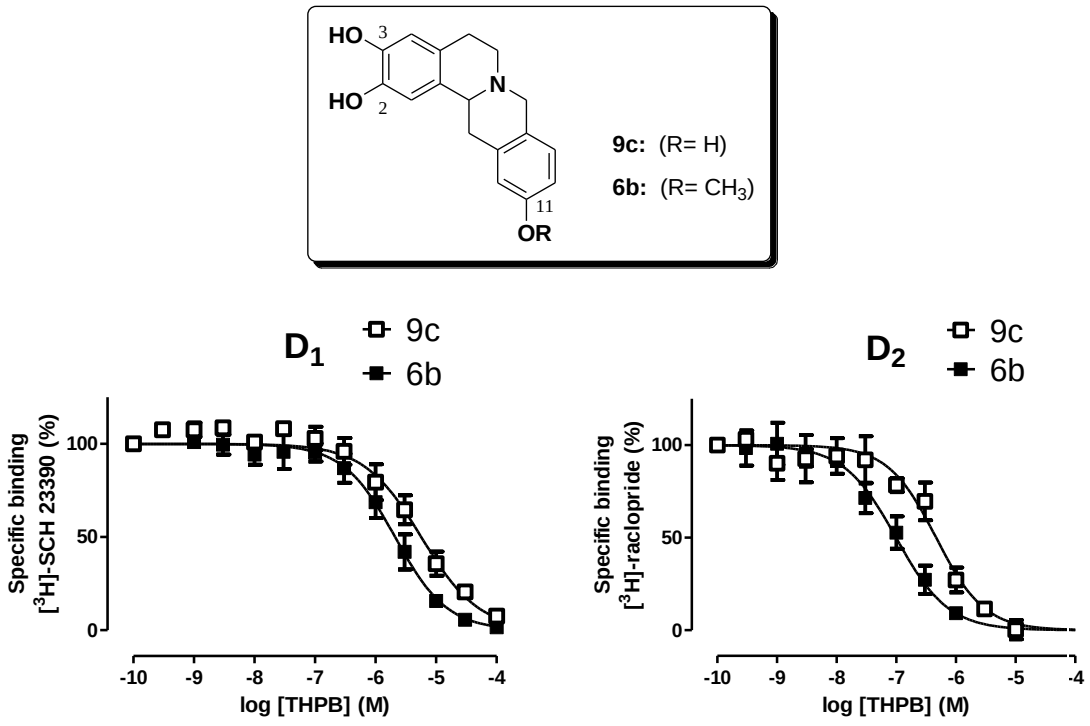

Figure 4. Displacement curves of the specific binding of D_1 and D_2 DR ligands by the compounds **6b** and **9c**. Data were displayed as mean ± SEM for 3-5 experiments.

2.3. Cytotoxicity studies

After determining the affinity for DRs of the synthesized THPBs, the potential cytotoxicity of these compounds was determined by the use of the MTT assay. The

concentrations tested were selected based on their respective Ki value for D_2 DR. None of the THPBs evaluated displayed any cytotoxicity on freshly isolated human neutrophils (**Figure 5**).

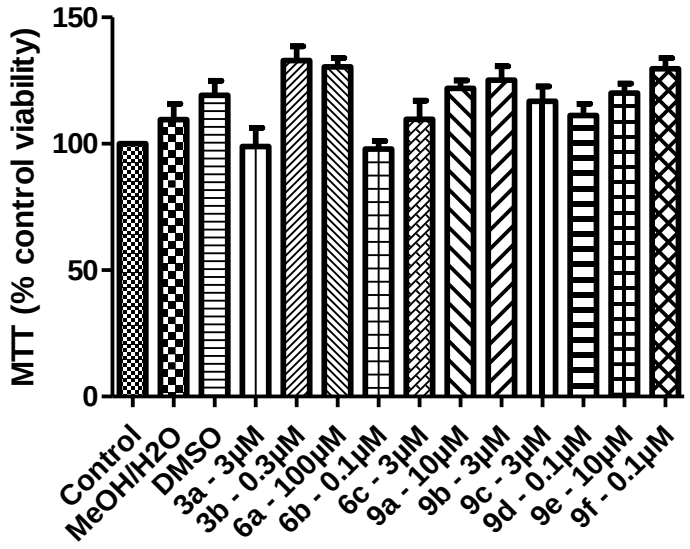

Figure 5. Effect of the synthesized THPBs on viability of human neutrophils. Data are presented as mean ± SEM of n=3 independent experiments.

To confirm the absence of toxicity, we next investigated the effect on neutrophil apoptosis and survival of the most active THPBs on D_2 DRs (**6b**, **9d** and **9f**). For this purpose a cytofluorimetric method was employed. As depicted in **Figure 6** none of the THPBs at the concentrations assayed affected neutrophil apoptosis or survival indicating the lack of human cell toxicity of these compounds in this in vitro approach.

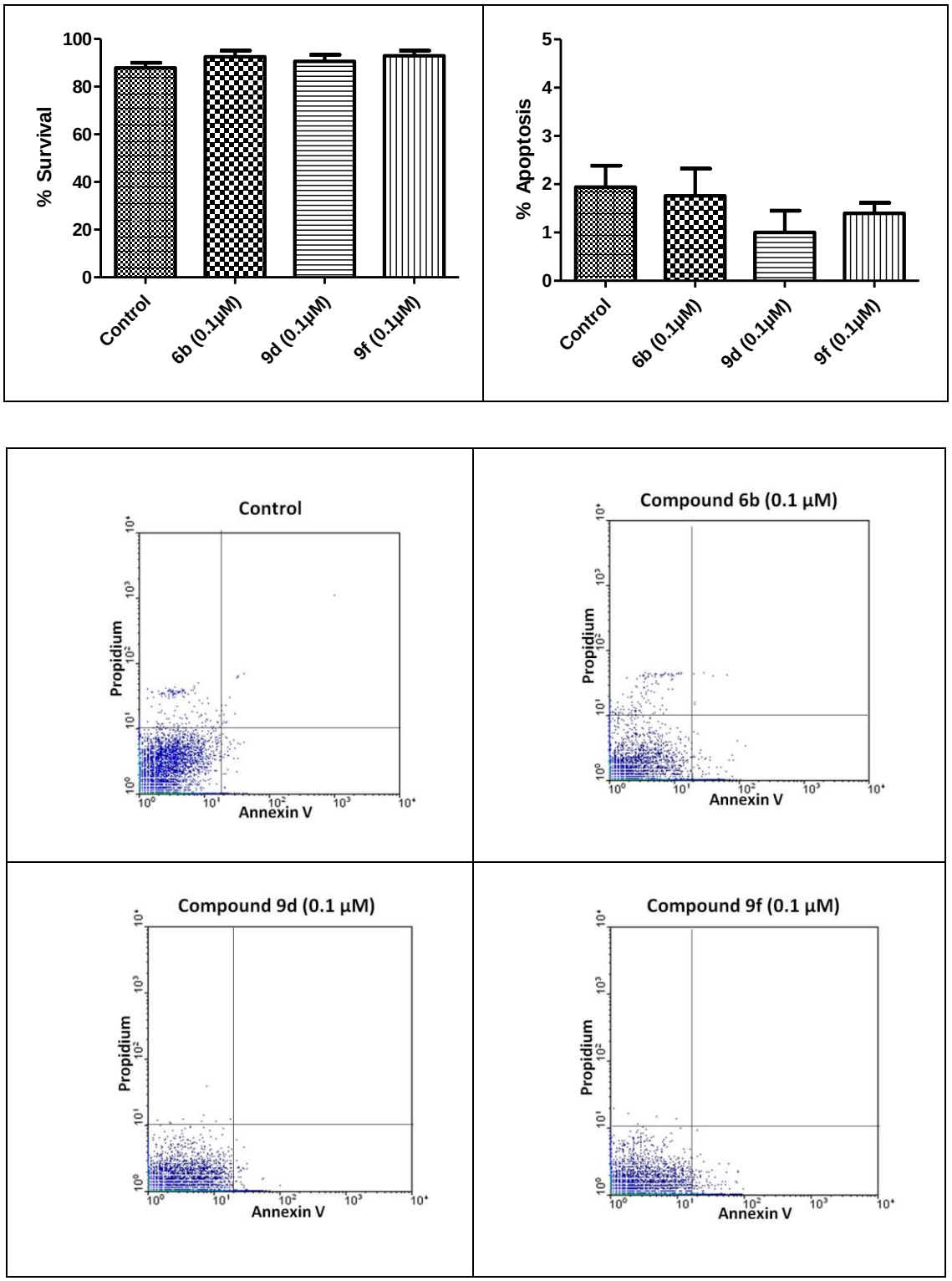

Figure 6. Percentage of apoptotic (A) and survival cells (B) after incubation with THPBs **6b**, **9d** and **9f**. Early apoptotic cells were quantified as the percentage of total population of annexin V+,PI− cells, late apoptotic, and/or necrotic cells as annexin V+ and PI+, and viable nonapoptotic cells as annexin V− and PI− at 24 h of culture of human neutrophils. The columns are the means ± SEM of n=3 independent experiments. Representative flow cytometry panels showing the effects of compounds **6b**, **9d** and **9f** on human neutrophil apoptosis have been included.

2.4. Molecular modeling

A molecular modeling study of three representative compounds of these series was performed to add further support to the results described in section 2.2. Special attention was paid to the effects exerted by the substituents into the D-ring of THPBs as well as to the increased affinity for the D_2 DR detected by the 11-*O*-protected derivatives. Therefore, compounds **9d**, **9c** and **6b** were selected for this comparative analysis due to their structural differences.

First, MD calculations were carried out simulating the molecular interactions between compounds **9d**, **9c** and **6b** with the human D_2 DR (**Figure 7**). In general, the three compounds displayed their pharmacophoric portions in a closely related spatial form to that reported for dopamine [17,18]. Consistent with previous experimental [36] and theoretical [37] data, the simulation indicated the relevance of the negatively charged aspartate 114 (D114) for ligand binding. In this contex, the highly conserved D114 in *trans*-membrane helix 3 (TM3) is important for both D_2 DR agonists and antagonists binding [36,38], and its terminal carboxyl group may function as an anchoring point for ligands with protonated amino groups [39-41]. In the current study, all the compounds simulated were docked into the receptor with the protonated amino group close to D114. Although after 5 ns of MD simulations the ligands slightly moved in a way different from the initial position, the strong interaction with D114 was maintained for all the complexes (see **Figure 7**), reinforcing the role of the amino acid as an anchoring point for ligands with protonated amino groups.

Next, the relative energies ($\Delta\Delta G$ values) obtained for the different complexes were analysed. A 0.00, 12.14 and 2.58 Kcal/mol for complexes **9d**/D_2DR, **9c**/D_2DR and **6b**/D_2DR, respectively were obtained. These binding energies (BE) were in agreement with the experimental data (see K_i values in **Table 1**). However, although BE allowed to

differentiate between very good and weak binders (0.00 kcal/mol for compound **9d** vs 12.14 kcal/mol for compound **9c**), those with similar binding affinities did not (0.0 kcal/mol for compound **9d** vs 2.58 kcal/mol for compound **6b**)**.** This was not surprising since MD simulations poorly approximate features that might be playing determinant roles such as lone pair directionality in hydrogen bonds, explicit π···π stacking polarization effects, hydrogen bonding networks, induced fit, and conformational entropy. Collectively, the information obtained from MD simulations might explain in part the differential D_2 DR affinity displayed by compounds **9d** and **9c**.

To acquire more detailed insights into the mechanisms driving the binding of the THPBs to the D_2 DR active site, the structure-affinity relationship was further analysed. The THPB-residue interaction spectra calculated by the free energy decomposition suggested that the interaction spectra of compounds **9d, 9c** and **6b** with D_2 DR was closely related. Nevertheless, some subtle but significant differences were detected reflecting differential binding features (**Figure 8**).

In this regard, it is interesting to note that the only structural difference between compounds **9d** and **9c** is the position of the OH groups in the D ring (see **Scheme 3**). Despite of it, a significant difference was obtained for their respective calculated BE, indicating that **9d**/D_2DR complex was markedly more stable than **9c**/D_2DR. The comparison of both spectra (**Figures 8a** and **8b**) revealed that the OH group of compound **9d** at position 9 (**Figure 8a**) was forming a strong hydrogen bond interaction with Y416. This is a particularly strong stabilizing interaction which is due to the acidic character of the oxygen atom of the Tyr residue. In contrast, the OH group of **9c**/D_2DR complex (**Figure 8b**), was located within a hydrophobic pocket where only weak hydrogen bonds (O….H-C with the side chains of the amino acids) can take place (see the weak stabilizing interaction with Y416, **Figure 8b**). In addition, although the

complex of compound **9c** displayed a moderated interaction with S193, there was not a stabilizing interaction with S197. This is in sharp contrast with **9d** spectra since two strong interactions with S193 and Ser197 were encountered (**Figure 8a**).

The remainder of the amino acids stabilizing these complexes (D114, V111 V115, C118, C182, I183, I184 W382, H393, F389, F390 and T412) exerted closelly related interactions. In ligth of these observations, it is tempting to speculate that the different stabilizing interactions of complexes **9d**/D_2 DR and **9c**/D_2DR could explain both the different ΔΔG values and the experimental affinities (**Table 1**).

On the other hand, when the activities of the 2,3,11-triOH-THPB (**9c**) and the protected 2,3-diOH-11-OMe-THPB (**6b**) were compared, an increased affinity for D_2 DR was exerted by the 11-*O*-protected derivative (**Table 1**). The analysis of the two spectra (**Figure 8b** and **8c**) showed that compound **6b** can establish two strong molecular interactions with two serine residues (S193 and S197). The average structures obtained for the complexes **9d**/ D_2DR, **9c**/D_2DR, and **6b**/D_2DR from the last ns of simulation are shown in **Figures 9a, 9b** and **9c,** respectively. The salt bridge between the protonated N-H group of BTHPs and the carboxyl group of D114 as well as the rest of the interactions previously discussed can be appreciated in this figure.

At this stage, the trend predicted for the MD simulations can be considered as certainly significant. However, it should be noted that we were dealing with relatively weak interactions and therefore MD simulations might underestimate such interactions. Therefore, reduced models were constructed to perform more accurate DFT calculations (B3LYP/6-·1G(d)). These calculations allowed to perform a QTAIM analysis for a further characterization of the most critical interactions for these ligands.

The main interactions of compound **9d** at the binding pocket and the interactions net obtained are illustrated in **Figure 10**. The OH-2 in the catecholic ring is acting as a

proton donor with S193 (ρ(rb)=0.0207 au) and as a proton acceptor with two amino acids, H393 (0.0187 au) and S194 (0.0012 au). The OH-3 behaves as a proton donor with S197 (0.0238 au) and is also involved in three weak C-H hydrogen bonds with S193, S194 and V115. The OH-9 possesses only one strong hydrogen bond with Y416 (0.0370 au). It is noteworthy that the hydrogen bonds between the catecholic hydroxyls (OH-2 and OH-3) with the serine residues (S193 and S194) are facilitated by the adequate spatial orientation of the molecule in which the atoms of rings A, B, C and D are making further interactions with other residues (**Figure 10**). These stabilizing interactions include the strong salt bridge between the ammonium group of **9d** with the carboxyl group of D114, the weaker C-H--S interaction with S118 and the C-H--π interactions with F389 and V115. These interactions are present with varying intensity in the three compounds here analyzed.

The main interactions of compound **9c** at the binding pocket are shown in **Figure 11**. To facilitate the description of the molecule interactions, this figure was divided in two and the interactions of the catecholic ring are illustrated in **Figure 11a**. The OH-2 establishes a hydrogen bond with the carbonyl oxygen of the backbone of S193 (0.0246 au) but not with the side chain oxygen as found for **9d**/D_2DR. It also acts as a proton acceptor with H393 (0.0147 au) and with a C-H bond of the side chain of S193 (0.0067 au). The OH-3 behaves as a proton acceptor for C-H interactions with F390 and V115 without proton donor activity with any residue except a very weak H--H contact with S197 (0.0016 au). In addition, this OH can establish two O--O interactions with the carbonyl oxygen at S193 and the hydroxyl at S197. Such interactions suggest that this hydroxyl group is weakly bond at the binding site compared with **9d**/D2DR complex. In fact, while the sum of electronic density of all OH-3 interactions in the binding site (∑ρ (rb)) is 0.0247 for compound **9c**, the value for compound **9d** was 0.0391 au. The

OH-11 is forming C-H--O type interactions with C182 (0.0031 au), I183 (0.0037 au) and F110 (0.0022 au), O--O type interactions with the carbonyl oxygen of backbone C182 (0.0044 au) and a weak H--H interaction with V91 (0.0019 au) (**Figure 11b**).

Figure 12 shows the main interactions of compound **6b** at the binding pocket. The interaction pattern of this compound shares similarities with those observed for compound **9d**. In fact, OH-2 and OH-3 are acting as proton donors with S193 (0.0340 au) and S197 (0.0308 au) and as proton acceptors with H393 (0.0064 au), I184 (0.0048 au), S193 (0.0114 au) and V115 (0.0065 au) (**Figure 12a**). OMe-11 is only forming two very weak hydrogen bonds with the C-H bonds of the side chain (ρ(rb) = 0.0015) and the backbone (0.0011au) of I183 (**Figure 12b**).The CH_3 group is interacting with C182 (C-H--S interaction (0.0039 au)), V91 (C-H interaction (0.0085 au)) as well as with F110 (H--H interaction (ρ(rb) = 0.0184 au). Taken together all these observations and the sum of the electronic density of all the interactions (0.0150 au), it can be concluded that the binding strength of OMe-11 to D_2DR is not relevant. In contrast, compound **6b** interactions seemed to be stronger when they are established between the catecholic hydroxyls and the serine residues. As oppose to the OH-11 of **9c** who remained almost fixed with the same orientation (**Figure 11b)**, the OMe-11 group in **6b** is rotating almost freely during the simulation for MD calculations. This is a striking observation which may account for **9c** and **6b** differential D_2DR affinitiesy. Finally, the QTAIM analysis seem to indicate that the increased affinities of compounds **9d** and **6b** compared with those of **9c** may rely on the stronger interactions established between the catecholic hydroxyls and the serine residues.

3. Conclusions

In summary, we have synthesized several THPBs with different substituents into their A- and D- rings and evaluated the SAR for their potential dopaminergic affinity. Three series of THPBs were obtained: 2,11-dihydroxy-3-chloro-THPBs (series 1), 2,3-dihydroxy-11-methoxy-THPBs (series 2) and 2,3,11-trihydroxy-THPBs and 2,3,9-trihydroxy-THPBs (series 3). Concerning to their affinity for DR: first, the presence of hydroxyls groups into the A-ring resulted in increased the DR affinity and, blockade of these groups blunted these responses; second, a halogen in the A-ring shifted the selectivity of the compound towards one of the DR investigated; third, while the presence of an OH at position 9 resulted in a positive effect on DR affinities, its localization at position 11 was surprisingly detrimental, and the blockade of this hydroxyl group at position 11 (MeO) reversed their DR affinity.

In addition, none of the compounds evaluated showed any cytotoxicity in freshly isolated human neutrophils. Finally, a molecular modeling study of three representative THPBs was carried out. The QTAIM analysis allowed a further understanding of the different experimental affinities obtained for compounds **9d, 9c** and **6b**. Since serine residues cluster seemed to be crucial for agonist binding and receptor activation, it is likely that compounds **9d** and **6b** displayed such capability.

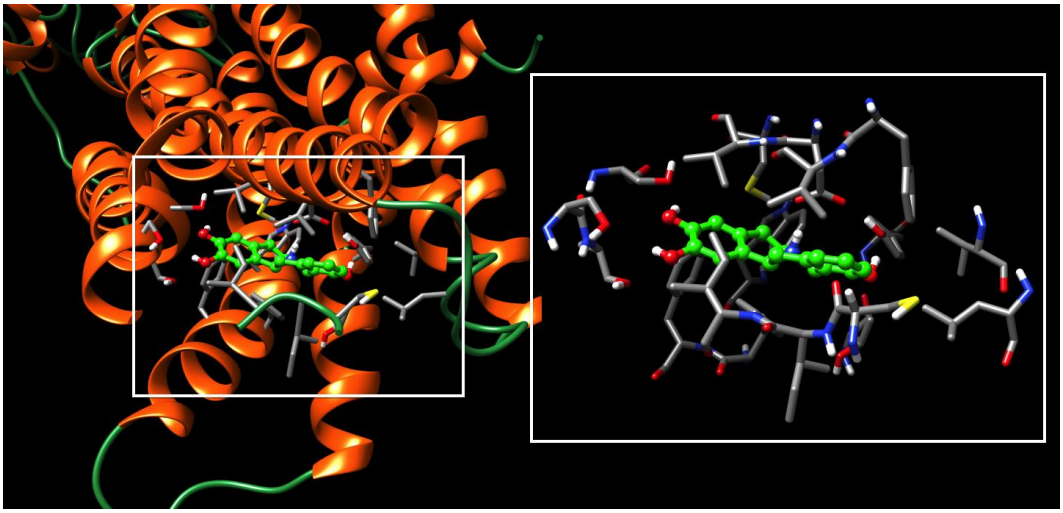

Figure 7. Spatial view of compound **9d** (green)/D_2DR interaction. Magnification of the receptor active site at the right.

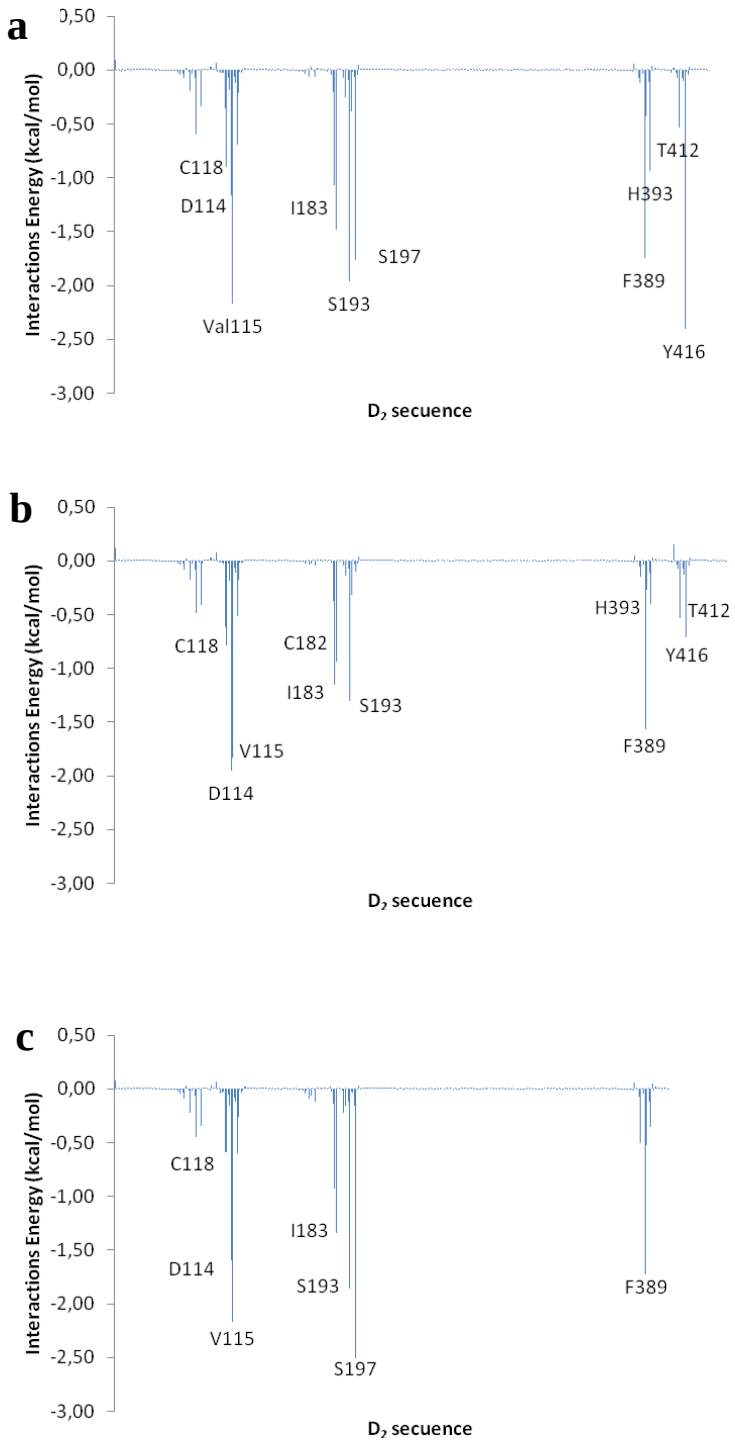

Figure 8. Histograms of interaction energies partitioned for D_2 DR amino acids when complexed with compound **9d (a),** compound **9c (b)** and compound **6b (c)**. The *x-axis* denotes the residue number of D_2 DR, and the *y-axis* shows the interaction energy between the compound and the specific residue. Negative and positive values represent favourable or unfavourable binding, respectively.

a

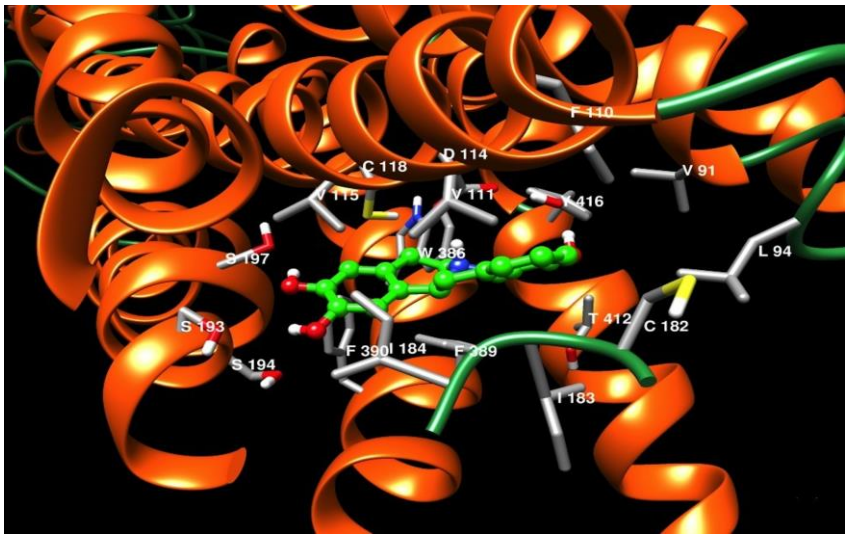

b

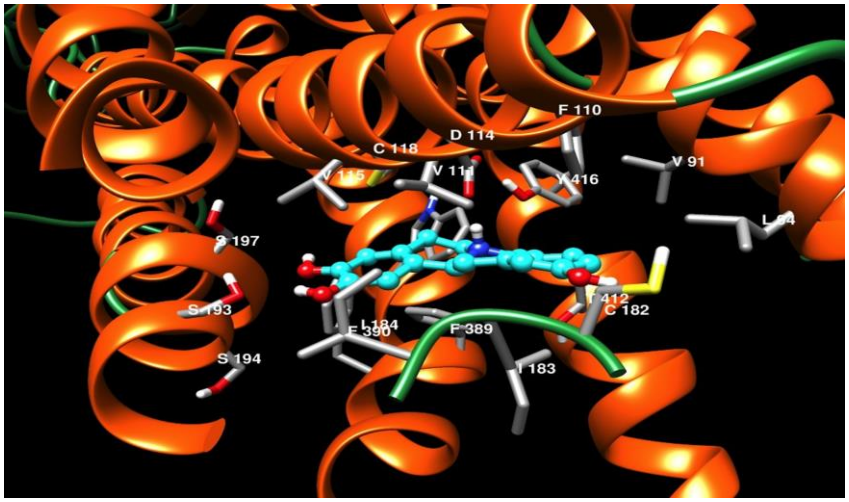

c

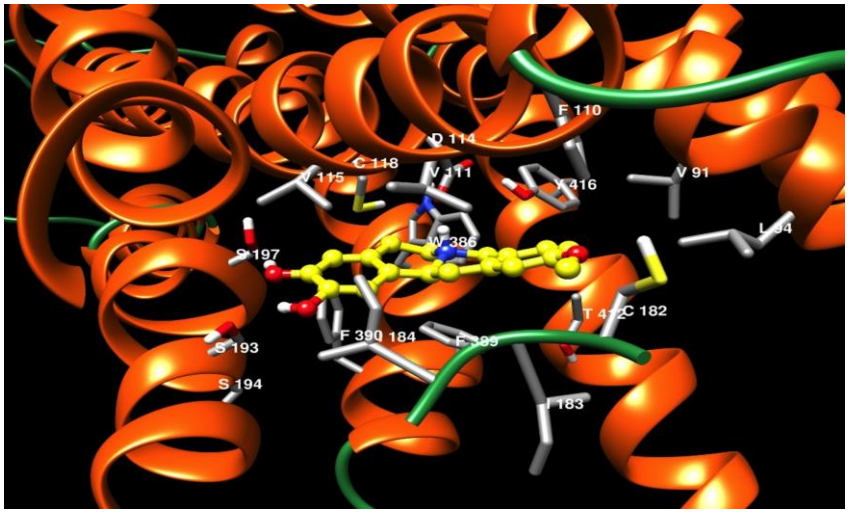

Figure 9. Spatial view of the active D2 DR site for compounds **9d (a), 9c (b**) and **6b (c)**. The names of the residues involved in the main interactions are written in the figure.

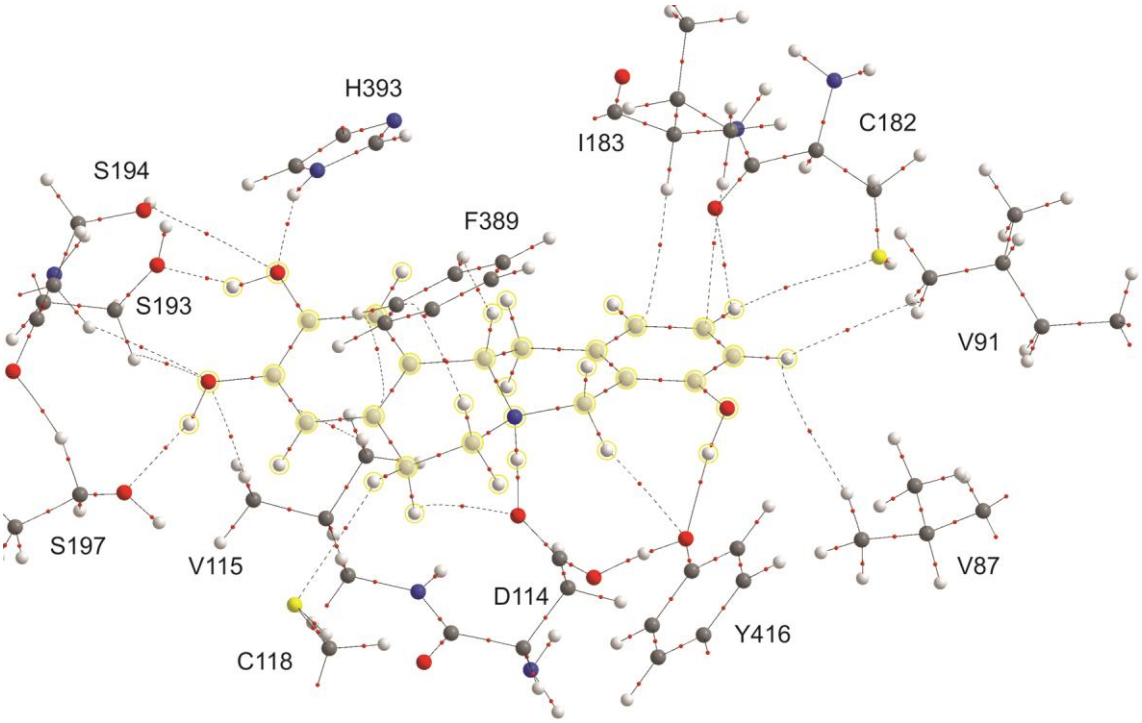

Figure 10. Molecular graph of compound **9d** interaction with the binding site. Large spheres represent attractors or nuclear critical points (3, -3) attributed to the atomic nuclei. The connecting nuclei lines are bond paths and small spheres on them are bond critical points (3, -1).

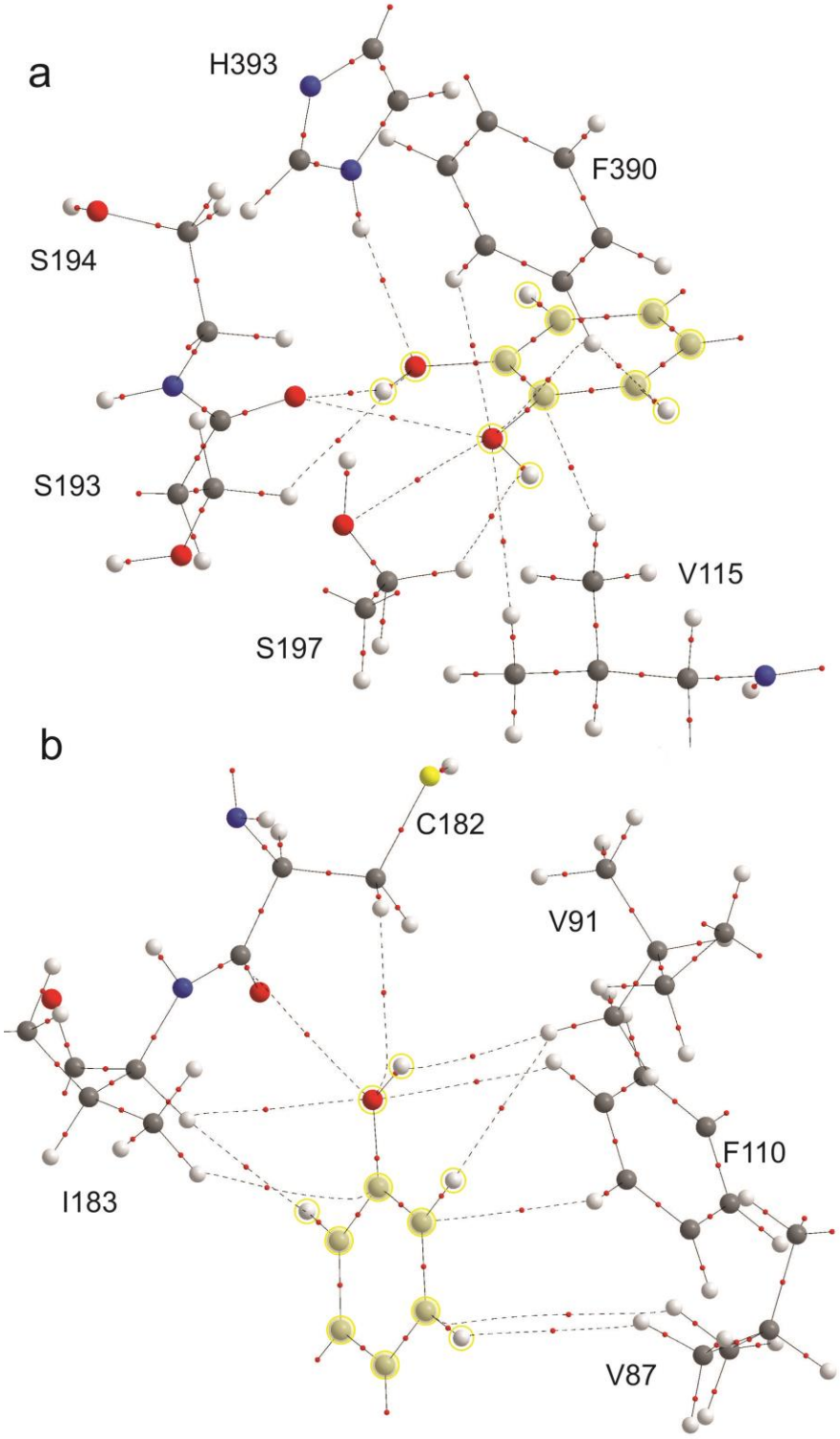

Figure 11. Molecular graph of compound **9c** interaction with the binding site. The interactions for the catecholic hydroxyls are shown in (**a**) and the interactions of OH-11 are shown in (**b**).

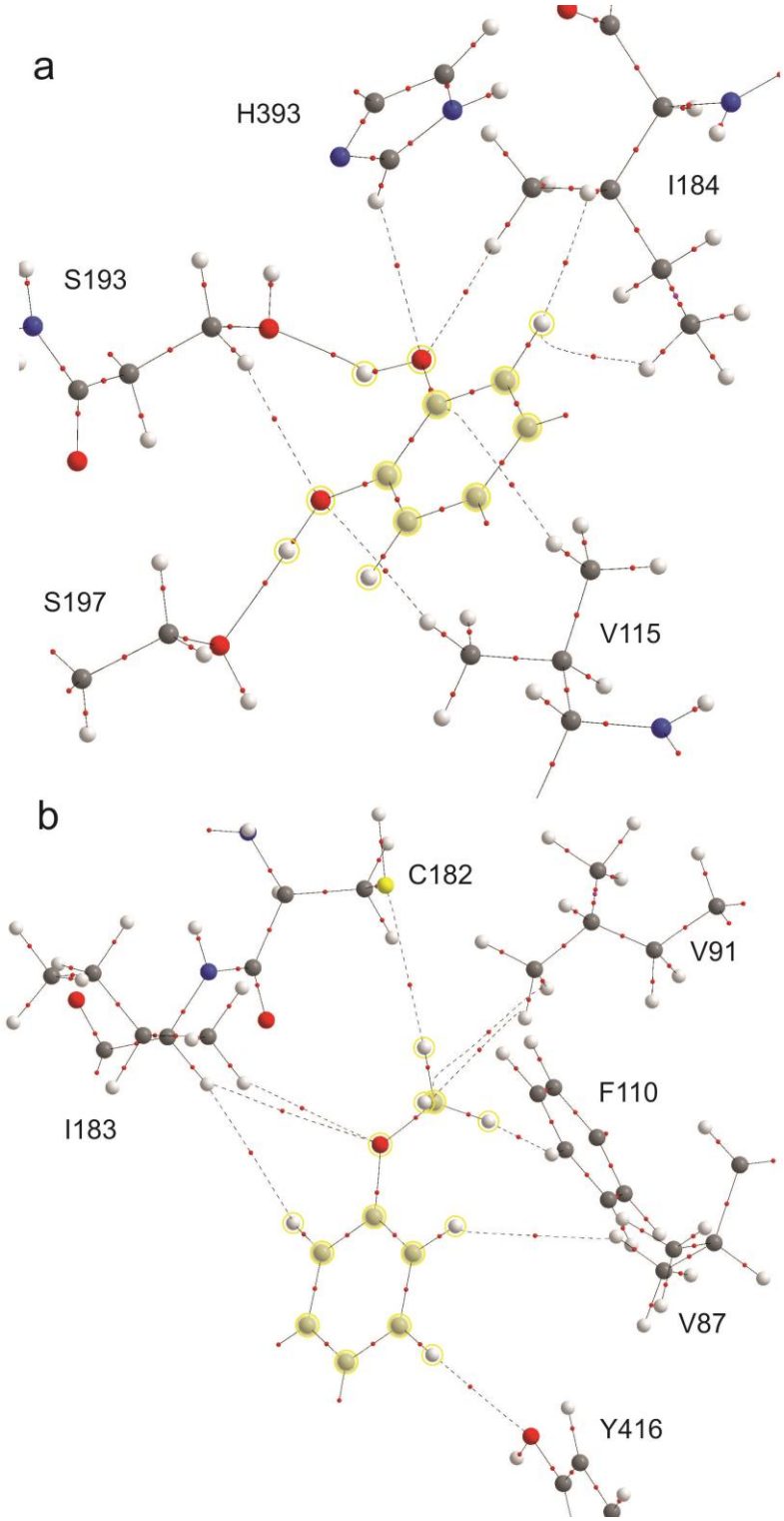

Figure 12. Molecular graph for compound **6b** interaction at the binding site. The interactions for the catecholic hydroxyls are shown in (**a**) and the interactions of OMe-11 are shown in (**b**).

4. Experimental Section

4.1. General Instrumentation

EIMS and FAB mass were recorded on a VG Auto Spec Fisons spectrometer instruments (Fisons, Manchester, United Kingdom). ^{1}H NMR and ^{13}C NMR spectra were recorded with $CDCl_3$ or C_5D_5N as a solvent on a Bruker AC-300, AC-400 or AC-500. Multiplicities of ^{13}C NMR resonances were assigned by DEPT experiments. COSY, HSQC and HMBC correlations were recorded at 400 MHz and 500 MHz (Bruker AC-400 o AC-500). The assignments of all compounds were made by COSY, DEPT, HSQC and HMBC. All the reactions were monitored by analytical TLC by silica gel 60 F_{254} (Merck 5554). Residues were purified by sílica gel 60 (40-63 μm, Merck 9385) column chromatography. Solvents and reagents used were purchased from commercial sources. Quoted yields are of purified material. The HCl salts of the synthesized compounds were prepared from the corresponding base with 5% HCl in MeOH.

4.2. Chemistry

4.2.1. General procedure for the synthesis of phenyethylamines (1 and 4).

4.2.1.1. 3,4-Dibenzyloxybenzaldehyde. A mixture of 3,4-dihydroxybenzaldehyde (1 g, 7.24 mmol), benzyl chloride (3 mL, 24.51 mmol) and anhydrous K_2CO_3 (2.1 g, 14.3 mmol) in absolute EtOH (15 mL) was refluxed for 6 h. After being stirred, the reaction mixture was concentrated to dryness, redissolved in 10 mL of CH_2Cl_2, and then 5% aqueous NaOH (3 x 10 mL) was added. The combined organic layers were dried over with anhydrous Na_2SO_4 and evaporated to dryness. The residue obtained was purified by silica gel column chromatography (Hexane/EtOAc, 8:2) to obtain the 3,4-dibenzyloxybenzaldehyde (1.5 g, 65%) as a white solid. ^{1}H NMR (500 MHz, $CDCl_3$):

δ= 9.83 (s, 1H, CHO), 7.56 (m, 2H, H-2, H-6), 7.48-7.27 (m, 10H, 2 x Ph), 7.02 (d, *J*= 13.7 Hz, 1H, H-5), 5.22 (s, 2H, $PhCH_2O$-3), 5.17 (s, 2H, $PhCH_2O$-4); ^{13}C NMR (125 MHz, $CDCl_3$) δ= 191.2 (CHO), 155.7 (C-4), 150.6 (C-3), 136.5 (C-1′), 136.3 (C-1″), 130.5 (C-1), 129-127 (6C, C-2′-4′ y C-2″-4″), 124.6 (CH-6), 116.9 (CH-5), 115.7 (CH-2), 71.3 ($PhCH_2O$-3), 71.1 ($PhCH_2O$-4); ESMS m/z (%): 341 $[M+Na]^+$, 313 (100).

4.2.1.2. 3-Chloro-4-methoxy-β-nitrostyrene. A mixture of 3-chloro-4-methoxy-benzaldehyde (1 g, 5.87 mmol), nitromethane (1 mL, 18.41 mmol) and NH_4OAc (1.2 g, 15.57 mmol) in AcOH (15 mL) was refluxed for 4 h. After this time, the reaction mixture was cooled to room temperature, diluted with H_2O (10 mL), and extracted with CH_2Cl_2 (3 x 10 mL). The combined organic layer were washed with brine (2 x 10 mL) and H_2O (2 x 10 mL), dried over with anhydrous Na_2SO_4, and evaporated to dryness to obtain the 3-chloro-4-methoxy-β-nitrostyrene (1.1 g, 88%) as yellow needles, which was used in the following step with no further purification. ^1H NMR (400 MHz, $CDCl_3$): δ= 7.91 (d, *J*= 13.7 Hz, 1H, H-β), 7.59 (d, *J*= 2.2 Hz, 1H, H-2), 7.52 (d, *J*= 13.7 Hz, 1H, H-α), 7.44 (dd, *J*= 8.6, 2.2 Hz, 1H, H-6), 6.97 (d, *J*= 8.6 Hz, 1H, H-5), 3.90 (s, 3H, OCH_3-4); ^{13}C NMR (100 MHz, $CDCl_3$) δ 158.4 (C-4), 138.4 (CH-β), 136.4 (CH-α), 130.9 (CH-2), 130.1 (CH-6), 124.2 (C-1), 123.7 (C-3), 112.7 (CH-5), 56.8 (OCH_3-4); MS (EI) *m/z* (%): 213 (55) $[M]^+$, 185 (100).

4.2.1.3. 3,4-Dibenzyloxy-β-nitrostyrene. 3,4-dibenzyloxybenzaldehyde (1 g, 3.15 mmol) was subjected to similar conditions to those above described to obtain the 3,4-dibenzyloxy-β-nitrostyrene (1.70 g, 99%) as yellow needles, which was used in the following step with no further purification. ^1H NMR (500 MHz, $CDCl_3$): δ= 7.81 (d, *J*= 13.6 Hz, 1H, H-β), 7.36 (d, *J*= 13.6 Hz, 1H, H-α), 7.38-7.23 (m, 10H, 2 x Ph), 7.01 (dd, *J*= 8.3, 2.1 Hz, 1H, H-6), 6.99 (d, J= 2.1 Hz, 1H, H-2), 6.87 (d, J= 8.3 Hz, 1H, H-5), 5.15 (s, 2H, $PhCH_2O$-3), 5.10 (s, 2H, $PhCH_2O$-4); ^{13}C NMR (125 MHz, $CDCl_3$) δ=

152.7 (C-4), 149.1 (C-3), 139.1 (CH-β), 136.4 (C-1′), 136.2 (C-1″), 135.3 (CH-α), 129–127 (6C, C-2′-4′ y C-2″-4″), 124.7 (CH-6), 123.1 (C-1), 114.3 (CH-2), 114.2 (CH-5), 71.4 ($PhCH_2O$-4), 70.8 ($PhCH_2O$-3); ESMS m/z (%): 362 (100) $[M+H]^+$.

4.2.1.4. β-(3-Chloro-4-methoxyphenyl)ethylamine (1). A solution of 3-chloro-4-methoxy-*β*-nitrostyrene (1 g, 4.7 mmol) in anhydrous THF (14 mL) was added dropwise to a well-stirred suspension of $LiAlH_4$ (0.7 g, 18.5 mmol) in anhydrous Et_2O (20 mL) under nitrogen atmosphere, and refluxed for 2 h. Then the reaction mixture was cooled and the excess reagent was destroyed by a dropwise addition of H_2O (2 mL) and 15% aqueous NaOH (5 mL). After a partial evaporation of the filtered portion, the aqueous solution was extracted with CH_2Cl_2 (3 x 10 mL) and the organic layer was extracted with 5% aqueous HCl (3 x 10 mL). The resulting aqueous acid layer was made basic (5% aqueous NH_4OH to achieve pH ≈ 9) and extracted with CH_2Cl_2 (3 x 10 mL). The organic layers were washed with brine (2 x 10 mL) and H_2O (2 x 10 mL), dried over with anhydrous Na_2SO_4 and concentrated to dryness to obtain the β-(3-chloro-4-methoxyphenyl)ethylamine (**1**) (630 mg, 72%) as a yellow oil. ^1H NMR (500 MHz, $CDCl_3$): δ= 7.33 (d, *J*= 2.2 Hz, 1H, H-2), 7.21 (dd, *J*= 8.5, 2.2 Hz, 1H, H-6), 6.88 (d, *J*= 8.5 Hz, 1H, H-5), 3.89 (s, 3H, OCH_3-4), 2.96 (m, 2H, H-β), 2.67 (m, 2H, H-α); ^{13}C NMR (125 MHz, $CDCl_3$): δ= 153.8 (C-4), 133.3 (C-1), 130.8 (CH-2), 128.4 (CH-6), 122.6 (C-3), 112.5 (CH-5), 56.5 (OCH_3-4), 43.8 (CH_2-β), 39.1 (CH_2-α); MS (EI) *m/z* (%): 185 (45) $[M]^+$.

4.2.1.5. β-(3,4-Dibenzyloxy-phenyl)ethylamine (4). 3,4-dibenzyloxy-β-nitrostyrene (1.70 g, 4.7 mmol) was subjected to similar conditions to those above described to obtain the β-(3,4-dibenzyloxyphenyl)ethylamine (**4**) (1.44 g, 93%) as a yellow oil. ^1H NMR (500 MHz, $CDCl_3$): δ= 7.47 (m, 4H, H-2′, H-6′ y H-2″, H-6″), 7.38 (m, 6H, H-3′, H-5′ y H-3″, H-5″), 6.83-6.76 (m, 3H, H-2, H-5, H-6), 5.16 (s, 2H,

$PhCH_2O$-3), 5.15 (s, 2H, $PhCH_2O$-4), 2.98 (m, 2H, CH_2-β), 2.83 (m, 2H, CH_2-α); ^{13}C NMR (125 MHz, $CDCl_3$): δ= 149.7 (C-3), 147.0 (C-4), 136.7 (C-1′), 136.6 (C-1″), 130.8 (C-1), 128.9-127.1 (6C, C-2′, C-4′ y C-2″,C-4″), 122.1 (CH-6), 112.8 (CH-2), 112.3 (CH-5), 121.9 (CH-6), 116.0 (CH-2), 112.8 (CH-4), 71.3 ($PhCH_2O$-4), 71.2 ($PhCH_2O$-3), 41.9 (CH_2-β), 39.3 (CH_2-α); ESMS m/z (%): 333 (100) $[M+H]^+$.

4.2.2. General procedure for the synthesis of acetamides (2, 5 and 8) under Schotten-Baumann conditions.

Formation of acetamides was carried out under Schotten-Baumann conditions using the appropriate phenylethylamine and the corresponding acid chloride.

4.2.2.1. *N*-(3-chloro-4-methoxyphenylethyl)-β-(3'-methoxyphenyl)acetamide (2). An amount of 0.3 mL of 2-(3-methoxyphenyl)acetyl chloride (2.55 mmol) was added dropwise at 0 ºC to a solution of *β*-(3-chloro-4-methoxyphenyl)ethylamine (**1**) (500 mg, 2.69 mmol) in CH_2Cl_2 (20 mL) and 5% aqueous NaOH (4.4 mL) with stirring at room temperature for 3 h. After the mixture was stirred, 2.5% aqueous HCl was added and the organic solution was washed with brine (2 x 10 mL) and H_2O (2 x 10 mL), dried over with anhydrous Na_2SO_4 and evaporated to dryness. The residue obtained was purified by sílica gel column chromatography (Hexane/CH_2Cl_2/EtOAc, 20:70:10) to afford the acetamide (**2**) (378 mg, 45%) as a white oil. ^1H NMR (500 MHz, $CDCl_3$): δ= 7.15 (t, *J*= 9.5 Hz, 1H, H-5′), 6.98 (d, *J*= 2.1 Hz, 1H, H-2), 6.74 (dd, *J*= 8.4, 2.1 Hz, 1H, H-6), 6.70 (dd, *J*= 9.5, 3.3 Hz, 1H, H-4′), 6.68 (m, 1H, H-5), 6.65 (m, 1H, H-6′), 6.62 (t, *J*= 3.3 Hz, 1H, H-2′), 5.50 (m, 1H, NH), 3.77 (s, 3H, OCH_3-4), 3.68 (s, 3H, OCH_3-3′), 3.33 (s, 2H, CH_2-CO), 3.31 (dd, *J*= 12.9, 6.8 Hz, 2H, H-α), 2.55 (t, *J*= 6.8 Hz, 2H, H-β); ^{13}C NMR (125 MHz, $CDCl_3$): δ= 170.7 (CO), 159.9 (C-3′), 153.5 (C-4), 136.1 (C-1′), 131.7 (C-1), 130.4 (CH-2), 130.0 (CH-5′), 127.9 (CH-6), 122.2 (C-3), 121.6 (CH-6′), 114.9 (CH-2′), 112.8 (CH-4′), 112.1 (CH-5), 56.1 (OCH_3-4), 55.1 (OCH_3-3′), 43.8

(CH_2-CO), 40.6 (CH_2-α), 34.3 (CH_2-β); MS (FAB) *m/z* (%): 356 $[M+Na]^+$, 186 (85), 169 (100).

4.2.2.2. *N*-(3,4-Dibenzyloxyphenylethyl)-β-(3'-methoxyphenyl)acetamide (5). *β*-(3,4-dibenzyloxyphenyl)ethylamine (500 mg, 1.5 mmol) was subjected to similar conditions to those above described to obtain the *N*-(3,4-dibenzyloxyphenylethyl)-β-(3'-methoxyphenyl)acetamide (**5**). The residue was purified by silica gel column chromatography (Hexane/CH_2Cl_2/ EtOAc, 20:70:10), to obtain the acetamide **5** (450 mg, 63%) as a white oil. ^{1}H NMR (500 MHz, $CDCl_3$): δ= 7.45-7.30 (m, 10H, Ph-3 y Ph-4), 7.20 (t, *J*= 8.0 Hz, 1H, H-5′), 6.80 (m, 1H, H-5), 6.80 (m, 1H, H-6′), 6.78 (m, 1H, H-2′), 6.72 (m, 1H, H-2), 6.72 (m, 1H, H-4′), 6.52 (dd, *J*= 8.1, 1.9 Hz, 1H, H-6), 5.43 (m, 1H, NH), 5.13 (s, 2H, $PhCH_2O$-4), 5.10 (s, 2H, $PhCH_2O$-3), 3.75 (s, 3H, OCH_3-3′), 3.47 (s, 2H, $NHCOCH_2$), 3.39 (q, *J*= 6.7 Hz, 2H, H-α), 2.63 (t, *J*= 6.7 Hz, 2H, H-β); ^{13}C NMR (125 MHz, $CDCl_3$): δ= 170.6 (CO), 159.9 (C-3′), 149.0 (C-3), 147.6 (C-4), 137.4 (C-1‴), 137.2 (C-1″), 136.2 (C-1′), 132.0 (C-1), 129.9 (CH-5′), 128.5-127.3 (10CH, Ph-3 y Ph-4), 121.6 (CH-6), 121.5 (CH-2′), 114.9 (CH-2), 114.9 (CH-4′), 112.8 (CH-5), 112.8 (CH-6′), 71.4 ($PhCH_2O$-4), 71.3 ($PhCH_2O$-3), 55.1 (OCH_3-3′), 43.8 ($NHCOCH_2$), 40.6 (CH_2-α), 34.8 (CH_2-β); MS (FAB) *m/z* (%): 504 $[M+Na]^+$, 413 (55), 322 (100).

4.2.2.3. *N*-(3,4-Dimethoxyphenylethyl)-β-(3'-methoxyphenyl)acetamide (8). 3,4-dimethoxy-phenylethylamine (500 mg, 2.79 mmol) was subjected to similar conditions to those above described to obtain the *N*-(3,4-dimethoxyphenylethyl)-β-(3'-methoxyphenyl)acetamide (**8**). The residue was purified by silica gel column chromatography (Hexane/CH_2Cl_2/ EtOAc, 20:70:10), to obtain the acetamide **8** (2 g, 91%) as a white oil. ^{1}H NMR (500 MHz, $CDCl_3$): δ= 7.21 (dd, *J*= 8.3, 7.9 Hz, 1H, H-5′), 6.80 (dd, *J*= 8.3, 1.9 Hz, 1H, H-4′), 6.73 (d, *J*= 7.9 Hz, 1H, H-6′), 6.72 (m, 1H, H-2′), 6.70 (d, *J*= 8.1 Hz, 1H, H-2), 6.60 (d, *J*= 1.9 Hz, 1H, H-5), 6.53 (dd, *J*= 8.1, 1.9 Hz, 1H,

H-6), 5.44 (m, 1H, NH), 3.85 (s, 3H, OCH_3-4), 3.81 (s, 3H, OCH_3-3), 3.76 (s, 3H, OCH_3-3′), 3.49 (s, 2H, $NHCOCH_2$), 3.43 (dd, *J*= 12.8, 6.8 Hz, 2H, H-α), 2.67 (t, *J*= 6.8 Hz, 2H, H-β); ^{13}C NMR (125 MHz, $CDCl_3$): δ= 170.7 (CO), 159.9 (C-3′), 148.9 (C-3), 147.6 (C-4), 136.2 (C-1′), 131.1 (C-1), 129.9 (CH-5′), 121.6 (CH-6′), 120.5 (CH-6), 114.9 (CH-2), 112.8 (CH-2′), 111.7 (C-4′), 111.2 (CH-5), 55.8 (OCH_3-4), 55.7 (OCH_3-3), 55.1 (OCH_3-3′), 43.9 ($COCH_2$), 40.7 (CH_2-α), 34.9 (CH_2-β); MS (FAB) *m/z* (%): 330 $[M+H]^+$, 182 (45), 165 (100).

4.2.3. Synthesis of 1,2,3,4-tetrahydroisoquinoleines (3, 6 and 9) by Bischler-Napieralski cyclisation.

4.2.3.1. 6-Chloro-7-methoxy-1-(3'-methoxybenzyl)-1,2,3,4-THIQ (3). The acetamide **2** (300 mg, 0.93 mmol) was added in dry toluene (10 mL) to a 100 mL three-neck round-bottom flask at 0 ºC under N_2 and treated with P_2O_5 (4.2 g, 15.02 mmol), which was added in portions and followed by the dropwise addition of $POCl_3$ (1.37 mL, 15.02 mmol). The mixture was stirred and refluxed under N_2 for 6 h, and then cooled to room temperature. Toluene was concentrated under reduced pressure and the reaction mixture was slowly poured into a mixture of crushed ice. The solid residue was triturated with 20 % aqueous NaOH to obtain a suspension (pH ≈ 8-9) and then extracted with CH_2Cl_2 (3 x 15 mL). The combined CH_2Cl_2 extracts were dried over Na_2SO_4 and the solvent was evaporated *in vacuo* obtaining a reddish oil. The residue was dissolved in MeOH (10 mL), cooled to -78 ºC and then treated with $NaBH_4$ (76 mg, 2 mmol). The reaction mixture was stirred for 2 h. Thereafter, H_2O (15 mL) was added and volatiles were evaporated under reduced pressure. The aqueous phase was extracted with CH_2Cl_2 (3 x 15 mL), and the combined organic layers were dried over with anhydrous Na_2SO_4 and evaporated to dryness. The crude product was purified by silica gel column chromatography (CH_2Cl_2/MeOH, 95:5) to furnish 6-chloro-7-methoxy-1-(3'-

methoxybenzyl)-1,2,3,4-THIQ (**3**) (155 mg, 54%) as a yellow oil. Then, the **3** hydrochloride salt was prepared for use in the next reaction. ^{1}H NMR (500 MHz, $CDCl_3$) for the free base form: δ= 7.25 (t, *J*= 7.5 Hz, 1H, H-5′), 7.10 (s, 1H, H-5), 6.83 (d, *J*= 7.5 Hz, 1H, H-6′), 6.80 (m, 1H, H-4′), 6.79 (m, 1H, H-2′), 6.64 (s, 1H, H-8), 4.18 (dd, *J*= 9.2, 4.7 Hz, 1H, H-1), 3.80 (s, 3H, OCH_3-7), 3.77 (s, 3H, OCH_3-3′), 3.17-2.92 (m, 4H, H-3 y CH_2-α), 2.71 (m, 2H, H-4); ^{13}C NMR (125 MHz, $CDCl_3$): δ= 159.8 (C-3′), 152.7 (C-7), 140.2 (C-1′), 137.8 (C-8a), 130.5 (CH-5), 129.6 (CH-5′), 128.2 (C-4a), 121.7 (CH-6′), 120.3 (C-6), 115.1 (CH-2′), 111.9 (CH-4′), 110.1 (CH-8), 56.9 (CH-1), 56.1 (OCH_3-7), 55.1 (OCH_3-3′), 42.6 (CH_2-α), 40.2 (CH_2-3), 28.7 (CH_2-4); MS (FAB) *m/z* (%): 318 $[M+H]^+$, 196 (100).

4.2.4. General procedure for the synthesis of 1,2,3,4-tetrahydroisoquinoleines (6 and 9) by Bischler-Napieralski cyclisation.

4.2.4.1. 6,7-Dibenzyloxy-1-(3'-methoxybenzyl)-1,2,3,4-THIQ (6). The corresponding acetamide **5** (300 mg, 0.645 mmol) was added in dry acetonitrile (20 mL) to a 100 mL three-neck round-bottom flask at 0 ºC under N_2, and treated with $POCl_3$ (0.45 mL, 4.5 mmol). The mixture was stirred and refluxed under N_2 for 5 h and then cooled to room temperature. Acetonitrile was concentrated under reduced pressure and the reaction mixture was slowly poured into a mixture of crushed ice. The solid residue was triturated with 10% aqueous NaOH to obtain a suspension (pH ≈ 8-9) which was then extracted with CH_2Cl_2 (3 x 15 mL). The combined CH_2Cl_2 extracts were dried over Na_2SO_4 and the solvent was evaporated *in vacuo* obtaining a reddish oil. The residue was dissolved in MeOH (10 mL), cooled to -78 ºC and then treated with $NaBH_4$ (76 mg, 2 mmol). The reaction mixture was stirred for 2 h. Next, H_2O (15 mL) was added and volatiles were evaporated under reduced pressure. The aqueous phase was extracted with CH_2Cl_2 (3 x 15 mL), and the combined organic layers were dried over Na_2SO_4 and

evaporated to dryness. The crude product was purified by silica gel column chromatography (CH_2Cl_2/MeOH, 95:5) to furnish THIQ (**6**) (180 mg, 63%) as a yellow oil. Then, the **6** hydrochloride salt was prepared for use in the next reaction. ^{1}H NMR (500 MHz, $CDCl_3$) for the free base form: δ= 7.45-7.30 (m, 10H, Ph-4 y Ph-3), 7.26 (m, 1H, H-5′), 6.81 (m, 1H, H-6′), 6.83 (m, 2H, H-2′, H-4′), 6.77 (s, 1H, H-5), 6.71 (s, 1H, H-8), 5.15 (s, 2H, $PhCH_2O$-4), 5.11 (s, 2H, $PhCH_2O$-3), 4.11 (dd, *J*= 9.5, 4.2 Hz, 1H, H-1), 3.81 (s, 3H, OCH_3-3′), 3.18 (m, 1H, H-3α), 3.10 (dd, *J*= 13.6, 4.2 Hz, 1H, H-α′), 2.91 (m, 1H, H-3β), 2.85 (dd, *J*= 13.6, 9.5 Hz, 1H, H-α″), 2.73 (m, 1H, H-4α), 2.69 (m, 1H, H-4β); ^{13}C NMR (125 MHz, $CDCl_3$): δ= 159.7 (C-3′), 147.6 (C-7), 146.8 (C-6), 140.6 (C-1′), 137.5 (C-1″), 137.4 (C-1‴), 131.4 (C-8a), 129.6 (CH-5′), 128.4-127.3 (10CH, Ph-6 y Ph-7), 127.9 (C-4a), 121.7 (CH-6′), 115.5 (CH-4′), 115.0 (CH-5), 113.9 (CH-2′), 111.8 (CH-8), 71.8 ($PhCH_2O$-7), 71.3 ($PhCH_2O$-6), 56.7 (CH-1), 55.1 (OCH_3-3′), 42.6 (CH_2-α), 40.7 (CH_2-3), 34.8 (CH_2-4); MS (FAB) *m/z* (%): 466 $[M+H]^+$, 344 (100).

4.2.4.2. 6,7-Dimethoxy-1-(3'-methoxybenzyl)-1,2,3,4-THIQ (9). *N*-(3,4-dimethoxy-phenyl-ethyl)-β-(3'-methoxyphenyl)acetamide (300 mg, 0.91 mmol) was subjected to similar conditions to those above described to obtain the 6,7-dimethoxy-1-(3'-methoxybenzyl)-1,2,3,4-THIQ (**9**). The residue was purified by silica gel column chromatography (CH_2Cl_2/ MeOH, 95:5), to afford the THIQ (**9**) (264 mg, 93%), as a yellow oil. Then, the **9** hydrochloride salt was prepared for use in the next reaction. ^{1}H NMR (500 MHz, $CDCl_3$) for the free base form: δ= 7.23 (dd, *J*= 7.6 Hz, 1H, H-5′), 6.83 (d, *J*= 7.6 Hz 1H, H-6′), 6.79 (m, 1H, H-2′), 6.77 (m, 1H, H-4′), 6.58 (s, 1H, H-5), 6.53 (s, 1H, H-8), 4.22 (dd, *J*= 8.5, 5.2 Hz, 1H, H-1), 3.84 (s, 3H, OCH_3-6), 3.77 (s, 3H, OCH_3-3′), 3.76 (s, 3H, OCH_3-7), 3.18 (dt, *J*= 12.0, 5.9 Hz 1H, H-3α), 3.16 (dd, *J*= 12.7, 5.2 Hz, 1H, H-α′), 2.99 (dd, *J*= 12.7, 8.5 Hz 1H, H-3β), 2.96 (m, 1H, H-α″), 2.78 (m, 2H, H-4); ^{13}C NMR (125 MHz, $CDCl_3$): δ= 159.7 (C-3′), 147.6 (C-6), 147.0 (C-7),

140.1 (C-1′), 129.6 (CH-5′), 129.2 (C-8a), 126.6 (C-4a), 121.7 (CH-6′), 115.1 (CH-2′), 111.9 (CH-5), 111.7 (CH-4′), 109.5 (CH-8), 56.5 (CH-1), 55.8 (OCH_3-3′), 55.8 (OCH_3-7), 55.1 (OCH_3-6), 42.5 (CH_2-α), 40.3 (CH_2-3), 28.7 (CH_2-4); MS (FAB) *m/z* (%): 314 $[M+H]^+$, 192 (100).

4.2.5. General procedure for the synthesis of tetrahydroprotoberberines (3a, 6a, 9a and 9b) by Mannich cyclisation.

4.2.5.1. 2,11-Dimethoxy-3-chlorotetrahydroprotoberberine (3a). The corresponding THIQ **3** (100 mg, 0.313 mmol) hydrochloride was added to a MeOH/ HCl 37% (20:1) (pH 1-4) solution placed in a 100 mL round-bottom flask and then evaporated to dryness. The compound was then dissolved in absolute ethanol (2 mL), H_2O (3 mL) and 37% aqueous formaldehyde (3 mL) and stirred and refluxed for 5 h. Thereafter, the reaction mixture was concentrated to dryness. The residue was basified with a 5% aqueous NaOH and the aqueous layer was extracted with CH_2Cl_2 (3 x 15 mL). The combined organic layers were dried over with anhydrous Na_2SO_4 and concentrated to dryness. The crude product was purified by silica gel column chromatography (Hexane/CH_2Cl_2/EtOAc, 20:70:10) to obtain THPB (**3a**) (85.4 mg, 0.26 mmol, 86%). ^{1}H NMR (500 MHz, $CDCl_3$): δ= 7.14 (s, 1H, H-4), 7.00 (d, *J*= 8.4 Hz, 1H, H-9), 6.75 (s, 1H, H-1), 6.73 (dd, *J*= 8.4, 2.5 Hz, 1H, H-10), 6.70 (d, *J*= 2.5 Hz, 1H, H-12), 3.98 (d, *J*= 14.5 Hz, 1H, H-8α), 3.91 (s, 3H, OCH_3-2), 3.79 (s, 3H, OCH_3-11), 3.70 (d, *J*= 14.5 Hz, 1H, H-8β), 3.64 (dd, *J*= 11.4, 3.6 Hz, 1H, H-14), 3.29 (dd, *J*= 16.2, 3.6 Hz, 1H, H-13α), 3.15 (m, 1H, H-6α), 3.10 (m, 1H, H-5α), 2.93 (dd, *J*= 16.2, 11.4 Hz, 1H, H-13β), 2.67 (m, 1H, H-5β), 2.60 (m, 1H, H-6β); ^{13}C NMR (125 MHz, $CDCl_3$): δ= 158.1 (C-11), 153.2 (C-2), 137.2 (C-14a), 135.1 (C-12a), 130.1 (CH-4), 127.7 (C-4a), 127.1 (CH-9), 126.3 (C-8a), 120.5 (C-3), 113.2 (CH-12), 112.4 (CH-10), 109.2 (CH-1), 59.5 (CH-14), 57.8 (CH_2-8), 56.3 (OCH_3-2), 55.2 (OCH_3-11), 50.9 (CH_2-6),

36.7 (CH_2-13), 28.3 (CH_2-5); MS (FAB) *m/z* (%): 330 $[M+H]^+$, 196 (100); HRMS-FAB $[M+H]^+$ calcd for $C_{19}H_{21}NO_2Cl$: 330.1255, found: 330.1262.

4.2.5.2. 2,3-Dibenzyloxy-11-methoxytetrahydroprotoberberine (6a). 6,7-dibenzyloxy-1-(3'-methoxybenzyl)-1,2,3,4-THIQ (**6**) (100 mg, 0.215 mmol) hydrochloride was subjected to similar conditions to those above described to obtain the 2,3-dibenzyloxy-11-methoxy-THPB (**6a**). The residue was purified by silica gel column chromatography (CH_2Cl_2/ MeOH, 99:1), to obtain THPB **6a** (93 mg, 93%) as a yellow oil. ^{1}H NMR (500 MHz, $CDCl_3$): δ= 7.45-7.30 (m, 10H, Ph-2 y Ph-3), 6.99 (d, *J*= 8.4 Hz, 1H, H-9), 6.83 (s, 1H, H-1), 6.75 (m, 1H, H-10), 6.72 (s, 1H, H-4), 6.68 (m, 1H, H-12), 5.16 (s, 2H, $PhCH_2O$-2), 5.12 (s, 2H, $PhCH_2O$-3), 3.95 (d, *J*= 14.4 Hz, 1H, H-8α), 3.79 (s, 3H, OCH_3-11), 3.63 (d, *J*= 14.4 Hz, 1H, H-8β), 3.53 (dd, *J*= 11.2, 3.5 Hz, 1H, H-14), 3.17 (dd, *J*= 16.3, 3.5 Hz, 1H, H-13α), 3.13 (m, 1H, H-6α), 3.10 (m, 1H, H-5α), 2.82 (dd, *J*= 16.3, 11.2 Hz, 1H, H-13β), 2.60 (m, 1H, H-5β), 2.58 (m, 1H, H-6β); ^{13}C NMR (125 MHz, $CDCl_3$): δ= 157.9 (C-11), 147.7 (C-2), 147.2 (C-3), 137.4 (C-1″), 137.2 (C-1′), 135.5 (C-12a), 130.6 (C-14a), 128.4-127.3 (8 x CH-Ph, CH-9), 127.0 (C-4a), 126.7 (C-8a), 114.9 (CH-4), 113.4 (CH-10), 113.2 (CH-1), 112.1 (CH-12), 72.2 ($PhCH_2O$-3), 71.1 ($PhCH_2O$-2), 59.4 (CH-14), 58.1 (CH_2-8), 55.2 (OCH_3-11), 51.4 (CH_2-6), 36.9 (CH_2-13), 28.9 (CH_2-5); MS (FAB) *m/z* (%): 478 $[M+H]^+$, 344 (100). HRMS-FAB $[M+H]^+$ calcd for $C_{32}H_{32}NO_3$: 478.2377, found: 478.2389.

4.2.5.3. 2,3,11-Trimethoxytetrahydroprotoberberine (9a) and 2,3,9-trimethoxy-tetrahydroprotoberberine (9b) by Mannich cyclisation. 6,7-dimethoxy-1-(3'-methoxybenzyl)-1,2,3,4-THIQ (**9**) (100 mg, 0.32 mmol) hydrochloride was subjected to similar conditions to those above described to obtain the 2,3,11-trimethoxy-THPB (**9a**) and 2,3,9-trimethoxy-THPB (**9b**). In this case, both compounds were obtained as a consequence the two possible cyclization positions: in *para* position to the

methoxyl group (THPB **9a**, major product) or in *ortho* position (THPB **9b**, minor product).

4.2.5.4. 2,3,11-Trimethoxytetrahydroprotoberberine (9a) was purified by silica gel column chromatography (Hexane/ EtOAc, 50:50, to obtain **9a** as a white oil (76 mg, 77%). ^{1}H NMR (500 MHz, $CDCl_3$): δ= 7.00 (d, *J*= 8.3 Hz, 1H, H-9), 6.74 (s, 1H, H-1), 6.72 (m, 1H, H-10), 6.70 (m, 1H, H-12), 6.62 (s, 1H, H-4), 3.97 (d, *J*= 14.5 Hz, 1H, H-8α), 3.89 (s, 3H, OCH_3-2), 3.86 (s, 3H, OCH_3-3), 3.78 (s, 3H, OCH_3-11), 3.66 (d, *J*= 14.5 Hz, 1H, H-8β), 3.58 (dd, *J*= 11.3, 3.5 Hz, 1H, H-14), 3.29 (dd, *J*= 16.2, 3.4 Hz, 1H, H-13α), 3.15 (m, 1H, H-6α), 3.15 (m, 1H, H-5α), 2.88 (dd, *J*= 16.2, 11.3 Hz, 1H, H-13β), 2.65 (m, 1H, H-5β), 2.60 (m, 1H, H-6β); ^{13}C NMR (125 MHz, $CDCl_3$): δ= 157.9 (C-11), 147.4 (C-2), 147.4 (C-3), 135.5 (C-12a), 129.6 (C-14a), 127.1 (CH-9), 126.7 (C-4a), 126.6 (C-8a), 113.2 (CH-12), 112.3 (CH-10), 111.3 (CH-4), 108.6 (CH-1), 59.5 (CH-14), 58.1 (CH_2-8), 56.0 (OCH_3-2), 55.8 (OCH_3-3), 55.2 (OCH_3-11), 51.4 (CH_2-6), 37.1 (CH_2-13), 29.0 (CH_2-5); MS (FAB) *m/z* (%): 326 $[M+H]^+$, 192 (100). HRMS-FAB $[M+H]^+$ calcd for $C_{20}H_{24}NO_3$: 326.1751, found: 326.1750.

4.2.5.5. 2,3,9-Trimethoxytetrahydroprotoberberine (9b) was purified by silica gel column chromatography (Hexane/ EtOAc, 50:50), to obtain **9b** as a yellow oil (8 mg, 0.0246 mmol, 8%). ^{1}H NMR (500 MHz, $CDCl_3$): δ= 7.15 (t, *J*= 7.9 Hz, 1H, H-11), 6.79 (d, *J*= 7.9 Hz, 1H, H-12), 6.75 (s, 1H, H-1), 6.70 (d, *J*= 7.9 Hz, 1H, H-10), 6.62 (s, 1H, H-4), 4.20 (d, *J*= 15.8 Hz, 1H, H-8α), 3.89 (s, 3H, OCH_3-2), 3.87 (s, 3H, OCH_3-3), 3.83 (s, 3H, OCH_3-9), 3.60 (dd, *J*= 11.1, 3.1 Hz, 1H, H-14), 3.46 (d, *J*= 15.8 Hz, 1H, H-8β), 3.30 (dd, *J*= 16.1, 3.1 Hz, 1H, H-13α), 3.20 (m, 1H, H-6α), 3.15 (m, 1H, H-5α), 2.90 (dd, *J*= 16.1, 11.1 Hz, 1H, H-13β), 2.65 (m, 1H, H-5β), 2.65 (m, 1H, H-6β); ^{13}C NMR (125 MHz, $CDCl_3$): δ= 155.8 (C-9), 147.4 (C-2), 147.4 (C-3), 135.8 (C-12a), 129.7 (C-14a), 126.8 (C-4a), 126.7 (CH-11), 123.4 (C-8a), 120.8 (CH-12), 111.4 (CH-4), 108.6

(CH-1), 107.1 (CH-10), 58.9 (CH-14), 56.0 (OCH_3-2), 55.8 (OCH_3-3), 55.2 (OCH_3-9), 53.7 (CH_2-8), 51.4 (CH_2-6), 36.9 (CH_2-13), 29.1 (CH_2-5); MS (FAB) *m/z* (%): 326 $[M+H]^+$, 192 (100); HRMS-FAB $[M+H]^+$ calcd for $C_{20}H_{24}NO_3$: 326.1751, found: 326.1754.

4.2.6. General procedure for the synthesis of THP 3b, 9c and 9d by *O*-demethylation.

4.2.6.1. 2,11-Dihydroxy-3-chloro-tetrahydroprotoberberine (3b). A solution of the appropriate THPB (**3a**) (50 mg, 0.15 mmol) in dry CH_2Cl_2 (5 mL) was cooled to -78 ºC. Then, BBr_3 (0.4 mL, 1.02 mmol) was dropwise added to the stirring solution. After 15 min, the reaction mixture was left to warm up to room temperature and stirred for 2 h. The reaction was terminated by the dropwise addition of MeOH (1 mL) and the mixture was further stirred for another 30 min. The solvent was concentrated to dryness. The crude product was purified by silica gel column chromatography (CH_2Cl_2:MeOH, 90:10), to obtain THPB (**3b**) (37 mg, 75%) as a yellow oil. ^{1}H NMR (500 MHz, C_5D_5N) δ= 7.22 (s, 1H, H-1), 7.18 (s, 1H, H-4), 7.05 (m, 1H, H-10), 7.03 (m, 1H, H-9), 6.96 (m, 1H, H-12), 3.99 (d, *J*= 14.3 Hz, 1H, H-8α), 3.61 (m, 1H, H-8β), 3.56 (m, 1H, H-14), 3.26 (dd, *J*= 16.1, 3.5 Hz, 1H, H-13α), 3.12 (m, 1H, H-5α), 3.06 (m, 1H, H-6α), 2.98 (dd, *J*= 16.1, 11.6 Hz, 1H, H-13β), 2.60 (m, 1H, H-5β), 2.52 (m, 1H, H-6β); ^{13}C NMR (125 MHz, C_5D_5N): δ= 157.1 (C-11), 152.6 (C-2), 138.1 (CH-14a), 135.9 (C-12a 8a), 130.0 (CH-4), 127.3 (CH-9), 126.7 (C-4a), 125.1 (C-12a), 119.6 (C-3), 115.7 (CH-12), 114.8 (CH-1), 114.4 (CH-10), 59.5 (CH-14), 57.9 (CH_2-8), 51.4 (CH_2-6), 36.9 (CH_2-13), 28.3 (CH_2-5); MS (FAB) *m/z* (%): 302 $[M+H]^+$, 182 (100); HRMS-FAB $[M+H]^+$ calcd for $C_{17}H_{17}NO_2Cl$: 302.0942, found: 302.0946.

4.2.6.2. 2,3,11-Trihydroxy-tetrahydroprotoberberine (9c). 2,3,11-trimethoxy-THPB (**9a**) (50 mg, 0.15 mmol) was subjected to similar conditions to those above

described to obtain the 2,3,11-trihydroxy-THPB (**9c**). The same equivalents of BBr_3 were employed despite the presence of increased methoxyl group numbers. The residue was purified by silica gel column chromatography (CH_2Cl_2/ MeOH, 90:10), to obtain the THPB **9c** (43 mg, 99%) as a white oil. ^{1}H NMR (500 MHz, C_5D_5N): δ= 7.15 (s, 1H, H-1), 7.01 (m, 1H, H-9), 7.00 (s, 3H, OH), 6.99 (m, 1H, H-12), 6.96 (s, 1H, H-4), 6.92 (m, 1H, H-10), 4.26 (d, *J*= 14.5 Hz, 1H, H-8α), 3.99 (d, *J*= 10.8 Hz, 1H, H-14), 3.91 (d, *J*= 14.5 Hz, 1H, H-8β), 3.37 (m, 1H, H-13α), 3.33 (m, 1H, H-5α), 3.32 (m, 1H, H-6α), 3.14 (m, 1H, H-13β), 2.89 (m, 1H, H-6β), 2.71 (m, 1H, H-5β); ^{13}C NMR (125 MHz, C_5D_5N): δ= 157.6 (C-11), 146.2 (C-2), 145.9 (C-3), 135.1 (C-12a), 127.5 (C-14a), 127.5 (CH-9), 124.5 (C-8a), 122.9 (C-4a), 116.1 (CH-4), 115.7 (CH-10), 114.7 (CH-12), 113.5 (CH-1), 59.7 (CH-14), 57.2 (CH-8), 51.4 (CH_2-6), 36.1 (CH_2-13), 27.8 (CH_2-5); MS (FAB) *m/z* (%): 284 $[M+H]^+$, 164 (100); HRMS-FAB $[M+H]^+$ calcd for $C_{17}H_{18}NO_3$: 284.1281, found: 284.1284.

4.2.6.3. 2,3,9-Trihydroxytetrahydroprotoberberine (9d). 2,3,9-trimethoxy-THPB (**9b**) (50 mg, 0.15 mmol) was subjected to similar conditions to those above described to obtain the 2,3,9-trihydroxy-THPB (**9d**). The residue was purified by silica gel column chromatography (CH_2Cl_2/ MeOH, 90:10), to obtain the THPB **9d** (42 mg, 97%) as a grey oil. ^{1}H NMR (500 MHz, C_5D_5N): δ= 7.21 (s, 1H, H-1), 7.11 (t, *J*= 7.8 Hz, 1H, H-11), 6.97 (s, 1H, H-4), 6.94 (d, *J*= 7.8 Hz, 1H, H-10), 6.71 (d, *J*= 7.8 Hz, 1H, H-12), 6.00 (s, 3H, OH), 4.71 (d, *J*= 15.7 Hz, 1H, H-8α), 3.97 (dd, *J*= 11.3, 3.4 Hz, 1H, H-14), 3.92 (d, *J*= 15.7 Hz, 1H, H-8β), 3.42 (dd, *J*= 16.4, 3.4 Hz, 1H, H-13α), 3.38 (m, 1H, H-5α), 3.36 (m, 1H, H-6α), 3.28 (dd, *J*= 16.4, 11.3 Hz, 1H, H-13β), 2.87 (m, 1H, H-6β), 2.68 (m, 1H, H-5β); ^{13}C NMR (125 MHz, C_5D_5N): δ= 154.9 (C-9), 146.1 (C-2), 145.9 (C-3), 135.9 (C-12a), 127.5 (CH-11), 124.9 (C-14a), 123.7 (C-8a), 122.9 (C-4a), 119.6 (CH-12), 116.1 (CH-4), 113.6 (CH-1), 112.6 (CH-10), 59.6 (CH-14), 54.0 (CH-8),

51.8 (CH_2-6), 36.4 (CH_2-13), 28.2 (CH_2-5); MS (FAB) *m/z* (%): 284 $[M+H]^+$, 164 (100); HRMS-FAB $[M+H]^+$ calcd for $C_{17}H_{18}NO_3$: 284.1281, found: 284.1282.

4.2.6.4. Synthesis of THP 6b by *O*-Debenzylation. A solution of 2,3-dibenzyloxy-11-methoxy-THPB (**6a**) (200 mg, 0.419 mmol) was refluxed for 3 h in absolute EtOH (25 mL) and concentrated HCl (25 mL). The reaction mixture was evaporated to dryness, redissolved in CH_2Cl_2 (10 mL) and made basic (15% aqueous NH_4OH). The organic solution was washed with brine (2 x 5 mL) and H_2O (2 x 5 mL), dried with anhydrous Na_2SO_4, and evaporated to dryness. The crude product was purified by silica gel column chromatography (CH_2Cl_2/MeOH 95:5) to obtain the 2,3-dihydroxy-11-methoxy-THPB (**6b**) (67 mg, 33%) as a yellow oil. ^{1}H NMR (500 MHz, $CDCl_3$): δ= 6.95 (d, *J*= 8.5 Hz, 1H, H-9), 6.70 (dd, *J*= 8.5, 2.4 Hz, 1H, H-10), 6.61 (d, *J*= 2.4 Hz, 1H, H-12), 6.51 (s, 1H, H-1), 6.20 (s, 3H, H-4, 2 x OH), 3.93 (d, *J*= 14.8 Hz, 1H, H-8α), 3.73 (s, 3H, OCH_3-11), 3.67 (d, *J*= 14.8 Hz, 1H, H-8β), 3.53 (dd, *J*= 11.2, 3.4 Hz, 1H, H-14), 3.08 (dd, *J*= 16.7, 3.4 Hz, 1H, H-13α), 3.03 (m, 1H, H-6α), 2.90 (m, 1H, H-5α), 2.76 (dd, *J*= 16.7, 11.2 Hz, 1H, H-13β), 2.57 (m, 1H, H-6β), 2.40 (m, 1H, H-5β); ^{13}C NMR (125 MHz, $CDCl_3$): δ= 158.3 (C-11), 143.6 (C-3), 143.5 (C-2), 134.9 (C-12a), 127.9 (C-14a), 127.1 (CH-9), 125.1 (C-4a), 124.9 (C-8a), 114.9 (CH-4), 113.5 (CH-12), 112.5 (CH-10), 111.9 (CH-1), 59.0 (CH-14), 57.4 (CH_2-8), 55.2 (OCH_3-11), 51.1 (CH_2-6), 35.4 (CH_2-13), 27.5 (CH_2-5); MS (FAB) *m/z* (%): 298 $[M+H]^+$, 164 (100); HRMS-FAB $[M+H]^+$ calcd for $C_{18}H_{20}NO_3$: 298.1438, found: 298.1439.

4.2.7. General procedure for the synthesis of THP 6c, 9e and 9f by formation of methylenedioxy group.

4.2.7.1. 2,3-Methylenedioxy-11-methoxytetrahydroprotoberberine (6c). A solution of 2,3-dihydroxy-11-methoxy-THPB (**6b**) (100 mg, 0.34 mmol) in anhydrous DMF (3 mL) was treated with dichloromethane (10 mL, 155.6 mmol) and CsF (250 mg,

1.64 mmol). The mixture was refluxed for 3 h with stirring. After cooling, the reaction mixture was extracted with CH_2Cl_2 and the organic layer was washed with 5% aqueous $NaHCO_3$ and H_2O, dried over with anhydrous Na_2SO_4 and concentrated *in vacuo* to dryness. The residue was purified by silica gel column chromatography (CH_2Cl_2/MeOH 95:5) to obtain the 2,3-methylendioxy-11-methoxy-THPB (**6c**) (90 mg, 86%) as a yellow oil. ^{1}H NMR (500 MHz, $CDCl_3$): δ= 6.99 (d, *J*= 8.4 Hz, 1H, H-9), 6.74 (s, 1H, H-1), 6.72 (dd, *J*= 8.4, 2.5 Hz, 1H, H-10), 6.68 (d, *J*= 2.5 Hz, 1H, H-12), 6.59 (s, 1H, H-4), 5.92 (s, 2H, OCH_2O), 3.95 (d, *J*= 14.4 Hz, 1H, H-8α), 3.79 (s, 3H, OCH_3-11), 3.65 (d, *J*= 14.4 Hz, 1H, H-8β), 3.57 (dd, *J*= 11.2, 3.5 Hz, 1H, H-14), 3.25 (dd, *J*= 16.3, 3.5 Hz, 1H, H-13α), 3.12 (m, 1H, H-6α), 3.09 (m, 1H, H-5α), 2.87 (dd, *J*= 16.3, 11.2 Hz, 1H, H-13β), 2.63 (m, 1H, H-5β), 2.60 (m, 1H, H-6β); ^{13}C NMR (125 MHz, $CDCl_3$): δ= 158.0 (C-11), 146.1 (C-2), 145.9 (C-3), 135.5 (C-12a), 130.8 (C-14a), 127.8 (C-4a), 127.1 (CH-9), 126.6 (C-8a), 113.2 (CH-12), 112.3 (CH-10), 108.4 (CH-4), 105.5 (CH-1), 100.7 (OCH_2O), 59.8 (CH-14), 58.0 (CH_2-8), 55.2 (OCH_3-11), 51.3 (CH_2-6), 37.2 (CH_2-13), 29.5 (CH_2-5); MS (FAB) *m/z* (%): 310 $[M+H]^+$, 176 (100); HRMS-FAB $[M+H]^+$ calcd for $C_{19}H_{20}NO_3$: 310.1438, found: 310.1440.

4.2.7.2. 2,3-Methylenedioxy-11-hydroxytetrahydroprotoberberine (9e). 2,3,11-trihydroxy-THPB (**9c**) (100 mg, 0.353 mmol) was subjected to similar conditions to those above described to obtain the 2,3-methylenedioxy-11-hydroxy-THPB (**9e**). The residue was purified by silica gel column chromatography (CH_2Cl_2/ MeOH, 98:2), to obtain the THPB **9e** (23 mg, 23%) as a white oil. ^{1}H NMR (500 MHz, C_5D_5N): δ= 7.06 (m, 3H, H-9, H-10, H-12), 6.90 (s, 1H, H-1), 6.63 (s, 1H, H-4), 5.96 (dd, *J*= 4.1, 1.2 Hz, 2H, OCH_2O), 4.00 (d, *J*= 14.3 Hz, 1H, H-8α), 3.62 (d, *J*= 14.3 Hz, 1H, H-8β), 3.57 (d, *J*= 11.4, 3.8 Hz, 1H, H-14), 3.33 (dd, *J*= 16.1, 3.8 Hz, 1H, H-13α), 3.12 (m, 1H, H-5α), 3.04 (m, 1H, H-6α), 2.99 (dd, *J*= 16.1, 11.4 Hz, 1H, H-13β), 2.58 (m, 1H, H-5β), 2.54

(m, 1H, H-6β); ^{13}C NMR (125 MHz, C_5D_5N): δ= 157.4 (C-11), 146.7 (C-2), 146.5 (C-3), 136.1 (C-12a), 131.3 (C-14a), 128.1 (C-4a), 127.5 (CH-9), 125.3 (C-8a), 115.8 (CH-12), 114.6 (CH-10), 108.7 (CH-4), 106.5 (CH-1), 101.3 (OCH_2O), 60.2 (CH-14), 58.1 (CH_2-8), 51.5 (CH_2-6), 37.3 (CH_2-13), 29.6 (CH_2-5); MS (FAB) *m/z* (%): 296 $[M+H]^+$, 176 (100); HRMS-FAB $[M+H]^+$ calcd for $C_{18}H_{18}NO_3$: 296.1281, found: 296.1282.

4.2.7.3. 2,3-Methylenedioxy-9-hydroxytetrahydroprotoberberine (9f). 2,3,9-trihydroxy-THPB (**9d**) (100 mg, 0.353 mmol) was submitted to the same conditions depicted above to obtain the 2,3-methylenedioxy-9-hydroxy-THPB (**9f**). The residue was purified by silica gel column chromatography (CH_2Cl_2/ MeOH, 98:2), to obtain the THPB **9f** (58 mg, 56%) as a white oil. ^{1}H NMR (500 MHz, C_5D_5N): δ= 7.16 (t, *J*= 7.8 Hz, 1H, H-11), 6.99 (d, *J*= 7.8 Hz, 1H, H-10), 6.95 (s, 1H, H-1), 6.84 (d, *J*= 7.8 Hz, 1H, H-12), 6.64 (s, 1H, H-4), 5.97 (dd, *J*= 4.9, 1.2 Hz, 1H, OCH_2O), 4.55 (d, *J*= 15.6 Hz, 1H, H-8α), 3.70 (d, *J*= 15.6 Hz, 1H, H-8β), 3.57 (dd, *J*= 11.1, 3.0 Hz, 1H, H-14), 3.38 (dd, *J*= 15.9, 3.0 Hz, 1H, H-13α), 3.12 (m, 1H, H-6α), 3.06 (m, 1H, H-5α), 3.01 (dd, *J*= 15.9, 11.1 Hz, 1H, H-13β), 2.54 (m, 1H, H-5β), 2.48 (m, 1H, H-6β); ^{13}C NMR (125 MHz, C_5D_5N): δ= 155.0 (C-9), 146.7 (C-2), 146.4 (C-3), 136.8 (C-12a), 131.8 (C-14a), 128.4 (C-4a), 127.1 (CH-11), 123.1 (C-8a), 119.8 (CH-12), 112.5 (CH-10), 108.7 (CH-4), 106.3 (CH-1), 101.2 (OCH_2O), 59.9 (CH-14), 54.8 (CH_2-8), 51.8 (CH_2-6), 37.7 (CH_2-13), 29.9 (CH_2-5); MS (FAB) *m/z* (%): 296 $[M+H]^+$, 176 (100); HRMS-FAB $[M+H]^+$ calcd for $C_{18}H_{18}NO_3$: 296.1281, found: 296.1280.

4.3. Bioassays

4.3.1. Binding experiments. These experiments were performed on striatal membranes. Each striatum was homogenized in 2 mL ice-cold Tris-HCl buffer (50 mM, pH = 7.4 at 22 ºC) with a Polytron (4s, maximal scale) and immediately diluted with

Tris buffer. The homogenate was centrifuged either twice ([^{3}H] SCH 23390 binding experiments) on four times ([^{3}H] raclopride binding experiments) at 20000g for 10 min at 4 ºC with resuspension in the same volume of Tris buffer between centrifugations. For [^{3}H] SCH 23390 binding experiments, the final pellet was resuspended in Tris buffer containing 5 mM $MgSO_4$, 0.5 mM EDTA and 0.02% ascorbic acid (Tris-Mg buffer), and the suspension was briefly sonicated and diluted to a protein concentration of 1 mg/mL. A 100µL aliquot of freshly prepared membrane suspension (100 µg of striatal protein) was incubated for 1h at 25 ºC with 100µL Tris buffer containing [^{3}H] SCH 23390 (0.25 nM final concentration) and 800µL of Tris-Mg buffer containing the required drugs. Non-specific binding was determined in the presence of 30 µM SK&F 38393 and represented around 2-3% of total binding. For [^{3}H] raclopride binding experiments, the final pellet was resuspended in Tris buffer containing 120 mM NaCl, 5 mM KCl, 1 mM $CaCl_2$, 1 mM $MgCl_2$ and 0.1% ascorbic acid (Tris-ions buffer), and the suspension was treated as described above. A 200 µL aliquot of freshly prepared membrane suspension (200 µg of striatal protein) was incubated for 1 h at 25 °C with 200 µL of Tris buffer containing [^{3}H] raclopride (0.5 nM, final concentration) and 400 µL of Tris-ions buffer containing the drug under investigation. Non-specific binding was determined in the presence of 50 µM apomorphine and represented around 5-7% of the total binding. In both cases, incubations were stopped by addition of 3 mL of ice-cold buffer (Tris-Mg buffer or Tris-ions buffer, as appropriate) followed by rapid filtration through Whatman GF/B filters. Tubes were rinsed with 3 mL of ice-cold buffer, and filters were washed with 3 x 3 mL ice-cold buffer. After the filters had been dried, radioactivity was counted in 4 mL BCS scintillation liquid at an efficiency of 45%. Filter blanks corresponded to approximately 0.5% of total binding and were not modified by drugs.

4.3.2. In vitro cytotoxicity studies. Cytotoxicity of the THPBs was studied by the use of two different in vitro approaches (MTT colorimetric assay and flow cytrometry analysis) [42]. Cytotoxicity was evaluated on freshly isolated human peripheral blood neutrophils. Human neutrophils were obtained from buffy coats of healthy donors by Ficoll-Hypaque density gradient centrifugation, as previously described [43]. Cultures were maintained at 37 ºC under 5% CO_2 and 95% air atmosphere in RPMI-1640 medium (Sigma–Aldrich Chemical, USA).

4.3.2.1. MTT assay. The viability of neutrophils was determined using the previously described MTT (3-(4,5-dimethylthiazol-2-yl)-2,5-diphenyltetrazolium bromide) colorimetric assay [44]. In this assay, the yellow MTT is reduced to a blue formazan product by the mitochondria of viable cells. MTT (Sigma–Aldrich) was prepared at 1 mg/mL in RPMI and stored at 4 ºC in the dark. 100 µl of neutrophils suspension (2 x 10^5 cells/mL) was added to each well of a 96-well microtiter plate followed by 20 µl of the appropriate concentration of the THPBs tested. The mixture was incubated at 37 ºC for 24 h. Then, 100 µl aliquot of MTT solution was added to each well and incubated at 37°C for another 60 min. The supernatants were discarded and 100 µl of DMSO was added to each well to dissolve the precipitated formazan. The optical densities at dual wavelengths (570 and 630 nm) were determined in a spectrophotometer (Infinite M200, Tecan, Mannedorf, Switzerland).

4.3.2.2. Cytofluorometric Analysis of Neutrophil Apoptosis and Survival. Freshly isolated neutrophils were resuspended in supplemented RPMI medium at 2 x 10^6 cells/mL. 25 µl were cultured in a 24-well plate containing 200 µl of supplemented RPMI medium for 24 h in the absence or presence of the most active THPBs on D_2 DR (**6b**, **9d** and **9f**). Assessment of apoptosis was performed by flow cytometry using annexin V- FITC and propidium iodide (PI). The protocol indicated by the manufacturer

(Annexin- Fluos; Roche Applied Science) was used as outlined previously [45]. Cells (1 x 10^4) were analyzed in a Beckman Coulter Epics XL (Fullerton, CA) and differentiated as early or viable apoptotic (annexin V^+ and PI^-), late apoptotic and/or necrotic (annexin V^+ and PI^+), and viable nonapoptotic (annexin V^- and PI^-) cells.

4.4. Molecular Modeling

4.4.1. Molecular dynamics simulations of complexes. A 3D model of the human D_2 DR was used for the MD simulations. This model is based on the homology model from the crystallized D_3 DR, β2 adrenoceptor and A2α adenosine receptor as templates [46].

(PMDB: http://mi.caspur.it/PMDB/codes: PM0077430).

The complex geometries from docking were soaked in boxes of explicit water using the TIP3P model [47] and subjected to MD simulation. All MD simulations were performed with the Amber software package using periodic boundary conditions and cubic simulation cells. The particle mesh Ewald method (PME) [48] was applied using a grid spacing of 1.2 Å, a spline interpolation order of 4 and a real space direct sum cutoff of 10 Å. The SHAKE algorithm was applied allowing for an integration time step of 2 fs. MD simulations were carried out at 300 K target temperature and extended to 10 ns overall simulation time. The NPT ensemble was employed using Berendsen coupling to a baro/thermostat (target pressure 1 atm, relaxation time 0.1 ps). Post MD analysis was carried out with program PTRAJ.

4.4.2. MM-GBSA free energy decomposition. In order to determine the residues of the D_2 DR active site involved in the interactions, the residues proposed by Andujar *et al.* [17] and Soriano-Ursua *et al.* were first identified. Then MM-GBSA free energy decomposition using the *mm_pbsa* program in AMBER12 was employed to corroborate the amino acids interacting with the ligands. This calculation can decompose the

interaction energies of each residue considering molecular mechanics and solvation energies [49,50]. Each ligand–residue pair includes four energy terms: van der Waals contribution (E_{vdw}), electrostatic contribution (E_{ele}), polar desolvation term (G_{GB}) and nonpolar desolvation term (G_{SA}), which are summarized in the following equation: $\Delta G_{inhibitor\text{-}residue} = \Delta E_{vdW} + \Delta E_{ele} + \Delta G_{GB} + \Delta G_{SA}$

For MM-GBSA methodology, snapshots were taken at 10 ps time intervals from the corresponding last 1000 ps MD trajectories and the explicit water molecules were removed from the snapshots.

4.4.3. Quantum mechanics calculations and topological study of the electron charge density distribution. 19 amino acids were included in this reduced model based on the generated data. Three molecular complexes, **9d**/D_2DR, **9c**/D_2DR and **6b**/D_2DR, obtained for our "reduced model system", were selected due to their reprensentative chemical feautures for the calculation of the charge density. Single point calculations were performed with Gaussian 03 and employing a hybrid B3LYP functional and 6-31G(d) as basis set. This type of calculation has been recently used in studies on the topology of $_{(r)}$ because it ensures a reasonable compromise between the wave function quality required to obtain reliable values of the derivatives of $_{(r)}$ and the computer power available, due to the extension of the system in study [17,18]. The topological properties of a scalar field such as $_{(r)}$ are summarized in terms of their critical points, i.e., the points r_c where $_{(r)} = 0$. Critical points are classified according to their type (,) by stating their rank, and signature. The rank is equal to the number of nonzero eigenvalues of the Hessian matrix of $_{(r)}$ at r_c, while the signature is the algebraic sum of the signs of the eigenvalues of this matrix. Critical points of (3, -1) and (3, +1) type describe saddle points, where the (3, -3) is the maximum and (3, +3) is the minimum in the field. Among these critical points, the (3,-1) or bond critical points are the most relevant ones since

they are found between any two atoms linked by a chemical bond. The determination of all the bond critical points and the corresponding bond paths connecting these point with bonded nuclei, were performed with the AIMAll software. The molecular graphs were drafted using the same program. Spatial views shown in **Figures 10** and **11** were constructed using the UCSF Chimera program as graphic interface.

It should be noted that the THPBs here reported were enantiomeric, they possessed one chiral center and they could raise two isomers (*S* and *R*). However, although an enantiomeric resolution for the biological assays was not carried out, only one isomer of each compound was evaluated in the calculations. The isomeric forms selected were first chosen on the basis of previously reported results [8-14] and on the exploratory simulations in which the spatially preferred form for these compounds was determined (results not shown). In this context, Sun *et al.* [23] showed that when a substituition was performed at the D ring, the S-isomers of THPBs displayed stronger affinities for the D_2 DR than their corresponding R-isomer. In addition, previous experimental findings with BTHIQs also supported this hypothesis since *S* forms were the preferred conformation of these compounds [13]. Finally, the preliminary and exploratory MD simulations peformed for the THPBs here synthesized revealed that the $\Delta\Delta G$ values obtained for the *R*-isomers are at least 10 Kcal/mol higher than their respective *S*-isomers. Therefore, the spatial conformationg adopted by the *S* forms seemed to provide the adequate orientation of the molecules for their interaction with the active site at the D_2 DR.

Acknowledgments

This study was supported by grants SAF2011-23777, Spanish Ministry of Economy and Competitiveness, RIER RD08/0075/0016, Carlos III Health Institute, Spanish Ministry of Health and the European Regional Development Fund (FEDER).

R.D.E. and S.A.A. are staff members of the National Research Council of Argentina (CONICET-Argentina).

References

[1] P.M. Luthra, J.B. Kumar, Plausible improvements for selective targeting of dopamine receptors in therapy of Parkinson's disease, J. Med. Chem. 14 (2012) 1556-1564.

[2] J.M. Beaulieu, R.R. Gainetdinov, The physiology, signaling, and pharmacology of dopamine receptors, Pharmacol. Rev. 63 (2011) 182-217.

[3] W. Poewe, Treatments for Parkinson disease-past achievements and current clinical needs, Neurology 72 (2009) S65-S73.

[4] N. Clausius, C. Born, H. Grunze, The relevance of dopamine agonists in the treatment of depression, Neuropsychiatry 23 (2009) 15-25.

[5] A.M. Basso, K.B. Gallagher, N.A. Bratcher, J.D. Brioni, R.B. Moreland, G.C. Hsieh, K. Drescher, G.B. Fox, M.W. Decker, L.E. Rueter, Antidepressant-like effect of D(2/3) receptor-, but not D(4) receptor-activation in the rat forced swim test, Neuropsychopharmacology 30 (2005) 1257-1268.

[6] M. Brocco, A. Dekeyne, M. Papp, M.J. Millan, Antidepressant-like properties of the anti-Parkinson agent, piribedil, in rodents: mediation by dopamine D2 receptors, Behav. Pharmacol. 17 (2006) 559-572.

[7] K. Kitagawa, Y. Kitamura, T. Miyazaki, J. Miyaoka, H. Kawasaki, M. Asanuma, T. Sendo, Effects of pramipexole on the duration of immobility during the forced swim test in normal and ACTH-treated rats, Naunyn Schmiedebergs Arch. Pharmacol. 380 (2009) 59-66.

[8] I. Berenguer, N. El Aouad, S. Andujar, V. Romero, F. Surive, T. Freret, A. Bermejo, M.D. Ivorra, R.D. Enriz, M. Boulouard, N. Cabedo, D. Cortes, Tetrahydroisoquinolines as dopaminergic ligands: 1-butyl-7-chloro-6-hydroxy-tetrahydroisoquinoline, a new compound with antidepressant-like activity in mice, Bioorg. Med. Chem. 17 (2009) 4968-4980.

[9] P. Protais, J. Arbaoui, E.H. Bakkali, A. Bermejo, D. Cortes, Effects of various isoquinoline alkaloids on in vitro 3H-dopamine uptake, J. Nat. Prod. 58 (1995) 1475-1484.

[10] A. Bermejo, P. Protais, M.A. Blázquez, K.S. Rao, M.C. Zafra-Polo, D. Cortes, Dopaminergic isoquinoline alkaloids from roots of *Xylopia papuana*, Nat. Prod. Lett. 6 (1995) 57-62.

[11] N. Cabedo, P. Protais, B.K. Cassels, D. Cortes, Synthesis and dopamine receptor selectivity of the benzyltetrahydroisoquinoline, (R)-(+)-nor-roefractine, J. Nat. Prod. 61 (1998) 709-712.

[12] I. Andreu, D. Cortes, P. Protais, B.K. Cassels, A. Chagraoui, N. Cabedo, Preparation of dopaminergic N-alkyl-benzyltetrahydroisoquinolines using a 'one-pot' procedure in acid medium, Bioorg. Med. Chem. 8 (2000) 889-895.

[13] N. Cabedo, I. Andreu, M.C. Ramírez de Arellano, A. Chagraoui, A. Serrano, B. Bermejo, P. Protais, D. Cortes, Enantioselective syntheses of dopaminergic (R)- and (S)-benzyltetrahydroisoquinolines, J. Med. Chem. 44 (2001) 1794-1801.

[14] I. Andreu, N. Cabedo, G. Torres, A. Chagraoui, M.C. Ramirez de Arellano, S. Gil, A. Bermejo, M. Valpuesta, P. Portais, D. Cortes, Syntheses of dopaminergic 1-cyclohexylmethyl-7,8-dioxygenated tetrahydroisoquinolines by selective heterogeneous tandem hydrogenation, Tetrahedron 58 (2002) 10173-10179.

[15] F.D. Suvire, N. Cabedo, A. Chagraoui, M.A. Zamora, D. Cortes, R.D. Enriz, Molecular recognition and binding mechanism of N-alkyl-benzyltetrahydroisoquinolines to the D_1 dopamine receptor. A computational approach. J. Mol. Struc. (Theochem) 666-667 (2003) 455-467.

[16] N. El Aouad, I. Berenguer, V. Romero, P. Marín, A. Serrano, S. Andujar, F. Suvire, A. Bermejo, M.D. Ivorra, R.D. Enriz, N. Cabedo, D. Cortes, Structure-activity relationship of dopaminergic halogenated 1-benzyl-tetrahydroisoquinoline derivatives, Eur. J. Med. Chem. 44 (2009) 4616-4621.

[17] S. Andujar, F. Suvire, I. Berenguer, N. Cabedo, P. Marín, L. Moreno, M.D. Ivorra, D. Cortes, R.D. Enriz, Tetrahydroisoquinolines acting as dopaminergic ligands. A molecular modeling study using MD simulations and QM calculations, J. Mol. Model. 18 (2012) 419-431.

[18] S.A. Andujar, R.D. Tosso, F.D. Suvire, E. Angelina, N. Peruchena, N. Cabedo, D. Cortes, R.D. Enriz, Searching the biologically relevant conformation of dopamine: a computational approach, J. Chem. Inf. Model. 52 (2012) 99-112.

[19] H. Xiao, J. Peng, Y. Liang, J. Yang, X. Bai, X.Y. Hao, F.M. Yang, Q.Y. Sun, Acetylcholinesterase inhibitors from *Corydalis yanhusuo*, Nat. Prod. Res. 25 (2011) 1418-1422.

[20] L. Slobodníková, D. Kostálová, D. Labudová, D. Kotulová, V. Kettmann, Antimicrobial activity of *Mahonia aquifolium* crude extract and its major isolated alkaloids, Phytother. Res. 18 (2004) 674-676.

[21] N. Cabedo, I. Berenguer, B. Figadère, D. Cortes, An overview on benzylisoquinoline derivatives with dopaminergic and serotonergic activities, Cur. Med. Chem. 16 (2009) 2441-2467.

[22] D. Cortes, J. Arbaoui, P. Protais, High affinity and selectivity of some tetrahydroprotoberberine alkaloids for rat striatal ^{3}H-raclopride binding sites, Nat. Prod. Lett. 3 (1993) 233-238.

[23] H. Sun, L. Zhu, H. Yang, W. Qian, L. Guo, S. Zhou, B. Gao, Z. Li, Y. Zhou, H. Jiang, K. Chen, X. Zhen, H. Liu, Asymmetric total synthesis and identification of tetrahydroprotoberberine derivatives as new antipsychotic agents possessing a dopamine D_1, D_2 and serotonin 5-HT_{1A} multi-action profile, Bioorg. Med. Chem. 21 (2013) 856-868.

[24] J. Dou, C. Tan, Y. Du, X. Bai, K. Wang, X. Ma, Effects of chitooligosaccharides on rabbit neutrophils in vitro, Carbohydr. Polym. 69 (2007) 209-213.

[25] M. Cheddadi, E. López-Cabarcos, K. Slowing, E. Barcia, A. Fernández-Carballido, Cytotoxicity and biocompatibility evaluation of a poly(magnesium acrylate) hydrogel synthesized for drug delivery, Int. J. Pharm. 413 (2011) 126-133.

[26] M.T. García, M.A. Blázquez, M.J. Ferrándiz, M.J. Sanz, N. Silva-Martín, J.A. Hermoso, A.G. de la Campa, New alkaloid antibiotics that target the DNA topoisomerase I of *Streptococcus pneumoniae*, J. Biol. Chem. 286 (2011) 6402-6413.

[27] G.W. Kabalka, R.S. Varma, Syntheses and selected reductions of conjugated nitroalkenes, Org. Prep. Proced. Int. 19 (1987) 283-328.

[28] C.M. Chen, Y.F. Fu, T.H. Yang, Synthesis of (±)-annonelliptine and (±)-anomoline, J. Nat. Prod. 58 (1995) 1767-1771.

[29] M. Shamma, The isoquinoline alkaloids: chemistry and pharmacology, Academic Press, New York, 1972.

[30] H.A. Ammar, Jr.P.L. Schiff, D.J. Slatkin, Synthesis of 7,7-dimethylaporphine alkaloids, Heterocycles 20 (1983) 451-454.

[31] T. Kametani, T. Kobari, K. Fukimoto, M. Fujihara, Studies on the synthesis of heterocycle compounds. Part CCCXCII. An alternative total synthesis of petaline, J. Chem. Soc. C (1971) 1796-1800.

[32] B.C. Uff, J.R. Kershaw, S.R. Chhabra, Reissert compound chemistry. Some rearrangement and substitution reactions, J. Chem. Soc. Perkin Trans. I (1972) 479-484.

[33] S. Doi, N. Shirai, Y. Sato, Abnormal products in the Bischler–Napieralski isoquinoline synthesis, J. Chem. Soc. Perkin Trans. I (1997) 2217-2221.

[34] R. Suau, M.V. Silva, M. Valpuesta, Structure and total synthesis of (-)-malacitanine. An unusual protoberberine alkaloid from *Ceratocapnos heterocarpa*, Tetrahedron 46 (1990) 4421-4428.

[35] M. Shamma, D.Y. Hwang, The synthesis of (±)-thalphenine, thaliglucine and thaliglucinona, Tetrahedron 30 (1974) 2279-2282.

[36] A. Manzour, F. Meng, J.H. Meador-Woodruff, L.P. Taylor, O. Civelli, H. Akil, Site directed mutagenesis of the human dopamine D_2 receptor, Eur. J. Pharm. Mol. Pharmacol. 227 (1992) 205-214.

[37] E. Hjerde, S.G. Dahl, I. Sylte, Atypical and typical antipsychotic drug interactions with the dopamine D_2 receptor, Eur. J. Med. Chem. 40 (2005) 185-194.

[38] W. Cho, L.P. Taylor, A. Mansour, A. Akil, Hydrophobic residues of the D_2 dopamine receptor are important for binding and signal transduction, J. Neurochem. 65 (1995) 2105-2115.

[39] D.A. Case, T.E. Cheatham, T. Darden, H. Gohlke, R. Luo, K.M. Merz, A. Onufriev, C. Simmerling, B. Wang, R.J. Woods, The amber biomolecular simulation programs, J. Comput. Chem. 26 (2005) 1668-1688.

[40] K.A. Neve, M.G. Cumbay, K.R. Thompson, R. Yang, D.C. Buck, V.J. Watts, C.J. Durand, M.M. Teeter, Modeling and mutational analysis of a putative sodium-binding pocket on the dopamine D_2 receptor, Mol. Pharmacol 60 (2001) 373-381.

[41] R.E. Wilcox, W.H. Huang, M.Y.K. Brusniak, D.M. Wilcox, R.S. Pearlman, M.M. Teeter, C.J. Durand, B.L. Wiens, K.A. Neve, CoMFA-based prediction of agonist affinities at recombinant wild type versus serine to alanine point mutated D_2 dopamine receptors, J. Med. Chem. 43 (2000) 3005-3019.

[42] L.E. Smith, S. Rimmer, S. MacNeil, Examination of the effects of poly(N-vinyl pyrrolidinone) hydrogels in direct and indirect contact with cells, Biomaterials 27 (2006) 2806-2812.

[43] C. Rius, M. Abu-Taha, C. Hermenegildo, L. Piqueras, J.M. Cerda-Nicolas, A.C. Issekutz, L. Estañ, J. Cortijo, E.J. Morcillo, F. Orallo, M.J. Sanz, Trans- but not cis-resveratrol impairs angiotensin-II-mediated vascular inflammation through inhibition of NF-κB activation and peroxisome proliferator-activated receptor-gamma upregulation, J. Immunol. 185 (2010) 3718-3727.

[44] M. Iacobini, A. Menichelli, G. Palumbo, G. Multari, B. Werner, D. Del Principe, Involvement of oxygen radicals in cytarabineinduced apoptosis in human polymorphonuclear cells, Biochem. Pharmacol. 61 (2001) 1033-1040.

[45] M.C. Martin, I. Dransfield, C. Haslett, A.G. Rossi, Cyclic AMP regulation of neutrophil apoptosis occurs via a novel protein kinase A-independent signaling pathway, J. Biol. Chem. 276 (2001) 45041-45050.

[46] M.A. Soriano-Ursua, J.O. Ocampo-Lopez, K. Ocampo-Mendoza, J.G. Trujillo-Ferrara, J. Correa-Basurto, Theoretical study of 3-D molecular similarity and ligand binding modes of orthologous human and rat D_2 dopamine receptors, Comput. Biol. Med. 41 (2011) 537-545.

[47] W.L. Jorgensen, J. Chandrasekhar, J.D. Madura, R.W. Impey, M.L. Klein, Comparison of simple potential functions for simulating liquid water, J. Chem. Phys. 79 (1983) 926-935.

[48] T. Darden, D. York, L. Pedersen, Particle mesh Ewald: an N·log(N) method for Ewald sums in large systems, J. Chem. Phys. 98 (1993) 10089-10092.

[49] T. Hou, N. Li, Y. Li, W. Wang, Characterization of domain-peptide interaction interface: prediction of SH3 domain-mediated protein-protein interaction network in yeast by generic structure-based models, J. Proteome Res. 11 (2012) 2982-2995.

[50] H. Gohlke, C. Kiel, D.A. Case, Insights into protein-protein binding by binding free energy calculation and free energy decomposition for the Ras-Raf and Ras-RalGDS complexes, J. Mol. Biol. 330 (2003) 891-913.

Figure captions

Figure 1. THPBs series.

Figure 2. Displacement curves of [^{3}H]-SCH 23390 (D_1) and [^{3}H] raclopride (D_2) specific binding by compounds **9d** and **9f**. Data were displayed as mean ± SEM for 3-5 experiments.

Figure 3. Displacement curves of the specific binding of D_1 and D_2 DR ligands by the compounds **9e** and **9f**. Data were displayed as mean ± SEM for 3-5 experiments.

Figure 4. Displacement curves of the specific binding of D_1 and D_2 DR ligands by the compounds **6b** and **9c**. Data were displayed as mean ± SEM for 3-5 experiments.

Figure 5. Effect of the synthesized THPBs on viability of human neutrophils. Data are presented as mean ± SEM of n=3 independent experiments.

Figure 6. Percentage of apoptotic (A) and survival cells (B) after incubation with THPBs **6b**, **9d** and **9f**. Early apoptotic cells were quantified as the percentage of total population of annexin V+,PI− cells, late apoptotic, and/or necrotic cells as annexin V+ and PI+, and viable nonapoptotic cells as annexin V− and PI− at 24 h of culture of human neutrophils. The columns are the means ± SEM of n=3 independent experiments. Representative flow cytometry panels showing the effects of compounds **6b**, **9d** and **9f** on human neutrophil apoptosis have been included.

Figure 7. Spatial view of compound **9d** (green)/D_2DR interaction. Magnification of the receptor active site at the right.

Figure 8. Histograms of interaction energies partitioned for D_2 DR amino acids when complexed with compound **9d (a),** compound **9c (b)** and compound **6b (c)**. The *x-axis* denotes the residue number of D_2 DR, and the *y-axis* shows the interaction energy between the compound and the specific residue. Negative and positive values represent favourable or unfavourable binding, respectively.

Figure 9. Spatial view of the active D2 DR site for compounds **9d (a), 9c (b**) and **6b (c)**.
The names of the residues involved in the main interactions are written in the figure.

Figure 10. Molecular graph of compound **9d** interaction with the binding site. Large spheres represent attractors or nuclear critical points (3, -3) attributed to the atomic nuclei. The connecting nuclei lines are bond paths and small spheres on them are bond critical points (3, -1).

Figure 11. Molecular graph of compound **9c** interaction with the binding site. The interactions for the catecholic hydroxyls are shown in (**a**) and the interactions of OH-11 are shown in (**b**).

Figure 12. Molecular graph for compound **6b** interaction at the binding site. The interactions for the catecholic hydroxyls are shown in (**a**) and the interactions of OMe-11 are shown in (**b**).

Scheme 1. Synthesis of THPBs **3a** and **3b** (Series 1). Reagents and Conditions: (a) Nitromethane, NH_4OAc, AcOH, reflux, 4h; (b) $LiAlH_4$, THF / Et_2O, N_2, reflux, 2h; (c) CH_2Cl_2, 3-methoxyphenylacetyl chloride, 5% NaOH, rt, 3h; (d) P_2O_5, $POCl_3$, Toluene, N_2, reflux, 8h; (e) $NaBH_4$; MeOH, rt, 2h; (f) HCHO, EtOH, H_2O, reflux, 5h; (g) CH_2Cl_2, BBr_3, rt, 2h.

Scheme 2. Synthesis of THPBs **6a-6c** (Series 2). Reagents and Conditions: (a) Benzyl chloride, K_2CO_3, EtOH, reflux, 6h; (b) Nitromethane, NH_4OAc, AcOH, reflux, 4h; (c) $LiAlH_4$, THF / Et_2O, N_2, reflux, 2h; (d) CH_2Cl_2, 3-methoxyphenylacetyl chloride, 5% NaOH, rt, 3h; (e) $POCl_3$, CH_3CN, N_2, reflux, 5h; (f) $NaBH_4$; MeOH, rt, 2h; (g) 37% HCHO, EtOH, H_2O, reflux, 5h; (h) EtOH-HCl, reflux, 3h; (i) DMF, CH_2Cl_2, CsF, reflux, 3h.

Scheme 3. Synthesis of THPBs **9a-9f** (Series 3). Reagents and Conditions: (a) CH_2Cl_2, 3-methoxyphenylacetyl chloride, 5% NaOH, rt, 3h; (b) $POCl_3$, CH_3CN, N_2, reflux, 5h; and, $NaBH_4$, MeOH, rt, 2h; (c) HCHO, EtOH, H_2O, reflux, 5h; (d) CH_2Cl_2, BBr_3, rt, 2h; (e) DMF, CH_2Cl_2, CsF, reflux, 3h.